INFORMATION TO USERS

This manuscript has been reproduced from the microfilm master. UMI films the text directly from the original or copy submitted. Thus, some thesis and dissertation copies are in typewriter face, while others may be from any type of computer printer.

The quality of this reproduction is dependent upon the quality of the copy submitted. Broken or indistinct print, colored or poor quality illustrations and photographs, print bleedthrough, substandard margins, and improper alignment can adversely affect reproduction.

In the unlikely event that the author did not send UMI a complete manuscript and there are missing pages, these will be noted. Also, if unauthorized copyright material had to be removed, a note will indicate the deletion.

Oversize materials (e.g., maps, drawings, charts) are reproduced by sectioning the original, beginning at the upper left-hand corner and continuing from left to right in equal sections with small overlaps. Each original is also photographed in one exposure and is included in reduced form at the back of the book.

Photographs included in the original manuscript have been reproduced xerographically in this copy. Higher quality 6" x 9" black and white photographic prints are available for any photographs or illustrations appearing in this copy for an additional charge. Contact UMI directly to order.

UMI

A Bell & Howell Information Company
300 North Zeeb Road, Ann Arbor MI 48106-1346 USA
313/761-4700 800/521-0600

Circular Dichroism and Fluorescence Spectroscopy Studies of the Protein Synthesis Initiation Factors with mRNA

By

Yahong Wang

A dissertation submitted to the Graduate Faculty in Chemistry in partial fulfillment of the requirements for the degree of Doctor of Philosophy,

The City University of New York

1996

This manuscript has been read and accepted for the Graduate Faculty in Chemistry in satisfaction of the dissertation requirement for the degree of Doctor of Philosophy.

2/12/96
Date

Chair of Examining Committee

4/9/96
Date

Executive Officer

Supervisory Committee

The City University of New York

Abstract

Circular Dichroism and Fluorescence Spectroscopy Studies of the Protein Synthesis Initiation Factors with mRNA

by

Yahong Wang

Advisor: Professor Dixie J. Goss

The structural features of wheat germ protein synthesis initiation factor eIF-(iso)4F, which has a cap binding protein as one of its two subunits, are unknown. In this study, circular dichroism (CD) spectra and secondary structure prediction were obtained for eIF-(iso)4F and its two subunits, p28 and p86. The α-helix content changed from 42% at pH 6.3 to 15% at pH 7.6, the optimum pH for cap binding. The β-sheet content increased from 14% at pH 6.3 to 38% at pH 7.6. The CD spectra of the two subunits, p28 and p86 were also measured and analyzed. The separated subunits both had a higher α-helix content at pH 7.6 than the native protein, giving values of 60% and 34% α-helix for p28 and p86, respectively. Binding of the dinucleotide cap analog to p28 reduced the α-helix content to approximately 8% with an increase in the β sheet content from 10% to 37%. In order to characterize the structural changes of wheat

germ protein synthesis initiation factor eIF-(iso)4F and p28 binding with mRNA cap analogs, CD spectroscopy was also performed on this system as a function of pH. The results reveal that the conformational changes in eIF-(iso)4F upon binding with mRNA are dependent on cap or oligonucleotide structure. A conformation consisting of approximately the same α-helix and β-sheet content can be induced by ligands even at non-optimal pHs. This large conformational transition suggests eIF-(iso)4F binds nucleic acids by interaction of a β-sheet motif and that these conformational transitions may have a regulatory role. The fluorescence stopped-flow studies of eIF-(iso)4F and p28 with cap show a concentration-independent conformational change. The rate of this conformational change was approximately ten fold faster for the isolated p28 compared to the native eIF-(iso)4F.

Recently the purified subunit p26, 26 kDa of wheat germ protein synthesis initiation factor eIF-4F has been obtained from *E. coli* expression of the cloned DNA. CD spectroscopy revealed 15% α-helix and 36% β-sheet in p26, and 38% α-helix and 17% β-sheet in eIF-4F. The binding of the 5'-terminal cap analog m^7GTP to p26 as a function of pH and temperature was described. The optimum binding pH was 8.0, ΔH and ΔS were 10.23 kcal/mol and 57.33 cal/mol°C, respectively. The environment of tryptophan residues in p26 and eIF-4F were monitored by using various quenchers. The results indicated the presence of negatively charged residues near the tryptophans

which were surrounded by a hydrophobic environment in p26 and eIF-4F. The stopped-flow kinetics demonstrated the interaction of eIF-4F with m^7GpppG cap analog followed a two-step mechanism. The rate constant and the activation energy for the second step were 121.7 s^{-1} and 4.55 kcal/mol, respectively.

Abbreviations

BME:	2-mercaptoethanol
CD:	circular dichroism
m^7G:	7-methylguanosine
eIF:	eukaryotic initiation factor
HEPES:	N-(2-hydroxyethyl)piperazine-N'-2-ethanesulfonic acid
DTT:	dithiothreitol
EDTA:	ethylenediaminetetraacetate
kDa:	kilodalton
PEG	polyethyleneglycol
Pipe:	1,4-Piperazinediethanesulfonic acid
PMSF	phenylmethylsulfonyl fluoride
SDS	sodium dodecyl sulfate
STI	soybean trypsin inhibitor
Tris	tris(hydroxymethyl)aminomethane

Acknowledgments

I would like to express my deep gratitude to my advisor, Dr. Dixie J. Goss, who maintained enthusiasm and support throughout this project. I am grateful to Dr. Max Diem and Dr. David C. Locke, who were most influential and agreed to served on my dissertation committee. Many thanks are extended to Dr. Kyoichi A. Wantanabe and Dr. Wu-Yun Ren, who graciously allowed me to utilize the CD instrument at the Sloan-Kettering Institute for Cancer Research. I am indebted to Dr. Karen S. Browning, whom we have pleasant collaboration with. I would also like to thank my colleagues, especially Dr. Ting Xiang, Dr. Luisa Balasta, Dr. Ma Sha, Yumin Gong, Xiaoxia Qian, Chin-chuan Wei, Tang Cheng, Minxue Huang, and Xiaosong Wang whom I learned from and worked with. Finally, I must thank to my parents, my brother and sister, and my husband, who have always encouraged me in pursuing my education. It is to them that this dissertation is dedicated.

Table of Contents

List of Tables

List of Figures

Chapter 3: Instrumentation

Chapter 4: pH-Dependent and Ligand Induced Conformational Changes of Eukaryotic Protein Synthesis Initiation Factors eIF-(iso)4F: Circular Dichroism and Stopped-flow Kinetic Studies

Chapter 5: Fluorescence and Circular Dichroism Spectroscopic Characterization of Wheat Germ Protein Synthesis Initiation Factor eIF-4F and its Subunit p26 with mRNA Cap Analogues

Chapter 1

Introduction

The mechanism and regulation of eukaryotic translation has been studied for many years. At a time when neither regulation nor mechanism were well understood, the results of Dr. Henshaw and his colleagues (1971) provided detailed analyses which demonstrated intermediates in the assembly of translation initiation complexes and regulation of polysome formation *in vivo*. Through many years investigation, a great deal is now known about the overall process of protein synthesis, yet the understanding of the details is poor. The exact role of protein synthesis initiation factors in facilitating the binding of the 40S subunit has not been elucidated. In an attempt to understand the molecular mechanism of protein synthesis and the interaction of proteins with mRNA, the system including two eukaryotic initiation factors eIF-4F, eIF-(iso)4F with mRNA cap analogs have been selected for this study.

Synthesis of proteins takes place in three stages: initiation, elongation and termination. Initiation involves the reactions that precede formation of the peptide bond between the first two amino acids of the protein. Elongation includes all the reactions from synthesis of the first peptide bond to addition of the last amino acid. Termination encompasses the steps that are needed to release the completed peptide chain; at the same time, the ribosome dissociates from the mRNA.

Initiation of protein synthesis in eukaryotes is a complex multistep process leading ultimately to the binding of the small ribosomal subunit to the mRNA and its proper

positioning on the initiator AUG (reviewed in Merrick, 1992). This event, which is considered rate limiting in translation (Jagus *et al.*, 1981), requires the participation of at least 12 initiation factors, several elongation factors and a release factor (reviewed in Rhoads, 1988 & 1991b; Hershey,1991; Kozak, 1988; and Sonenberg, 1988 & 1993) as well as mRNA, tRNA and ribosomes. The basic elements of the initiation of translation pathway are the association of factors with the ribosomal subunits to provide for a pool of 40S subunits with which to start the initiation pathway. This is accomplished primarily into three steps.

1. Ribosome dissociation:

The 80S eukaryotic ribosome dissociates into 40S and 60S subunits by the association of eukaryotic initiation factors eIF-2, eIF-3, eIF-4C and eIF-6 to provide for a pool of 40S subunits with which to start the initiation pathway.

2. mRNA binding:

A ternary complex (eIF-2•GTP•Met-tRNA$_i$) is formed and subsequently associated with the 40S subunit, to which 5' end of mRNA activated by eIF-4A, eIF-4B and eIF-4F (and eIF-(iso)4F in wheat germ) is bound. The initial 40S-mRNA complex is formed.

3. Ribosome joining:

Following the hydrolysis of the bound GTP in the ternary complex (eIF-2•GTP•Met-$tRNA_i$) triggered mainly by an interaction of eIF-5, factors are released from the 40S subunit and the 60S subunit joins yielding the 80S initiation complex to start protein synthesis.

A common structural feature of all cellular eukaryotic mRNAs (except for organelle mRNAs) analyzed to date is the presence of a 5'-terminal m^7GpppN (where N is any nucleotide) structure, termed the cap (Shatkin, 1985). m^7G cap is required for efficient mRNA translation and plays a prominent role in translational control (Furuichi *et al.*, 1977; Konarska *et al.*, 1984; Edery *et al.*, 1985 & Hart *et al.*, 1985). This structure is added early during the transcription of RNA polymerase II genes in the nucleus and is required for several steps of mRNA biogenesis which include (Edery *et al.*, 1995) (1) protecting the mRNA against 5' exonucleases, (2) stimulating translation, (3) stimulating precursor mRNA splicing, (4) enhancing nucleocytoplasmic transport, and (5) facilitating 3'-end processing. Cap analogs inhibit protein-RNA complex formation in a non-specific manner: inhibit translation of capped RNAs by decreasing 40 S ribosomal subunit binding to mRNAs. It was therefore concluded that the cap analogs competitively inhibit the function of one or more proteins required for translation initiation by saturating their cap interacting sites. The best-characterized role of the cap structure is its stimulatory effect on ribosome binding (reviewed in Rhoads, 1991 &

Sonenberg, 1991). Binding of the ribosomes to the mRNA is thought to be rate-limiting (Jagus *et al.*, 1981) and discriminatory step (Ray *et al.*, 1983).

The function of the cap structure in ribosome binding is mediated by the eukaryotic initiation factor-4 group, eIF-4A, eIF-4B and eIF-4F which is an ATP-dependent process and which in part results in the unwinding of mRNA secondary structure at or near the 5' m^7G cap structure (reviewed in Merrick, 1994 & Edery, *et al.*, 1987). eIF-4A is a prototype of a large family of RNA helicases. It is a 50 kDa polypeptide that exhibits RNA-dependent ATPase activity (Grifo *et al.*, 1984) and in conjunction with eIF-4B, RNA helicase activity (Rozen *et al.*,1990; Pause & Sonenberg,1992). eIF-4F is a three subunit complex that consists of cap binding p26 subunit, eIF-4A and p220 (eIF-4γ). p220 subunit migrates aberrantly with an Mr of 220 kDa, but whose cDNA encodes only a 150 kDa polypeptide (Grifo *et al.*, 1983). The function of p220 is not understood. However, an intact p220 subunit appears essential for eIF-4F function on cellular mRNAs. eIF-4F also exhibits RNA-dependent ATPase activity, and in conjunction with eIF-4B, RNA helicase activity that is 20 times more active than that of free eIF-4A (Ray *et al.*, 1985). Although the biochemical processes which the eukaryotic cell undertakes have been studied extensively *in vitro* with purified components, the mechanism by which initiation of translation occurs and is regulated is not well understood. Recently Rhoads *et al.* (1994) proposed a model for mRNA binding to the ribosome. eIF-4E interacts with the cap of mRNA prior to binding of

either component to the ribosome. eIF-4γ (p220) is present on the 43S initiation complex and provides a binding site for the eIF-4E:mRNA complex. This model gives a mechanism by which changes in the phosphorylation of eIF-4E could directly affect the overall rate of protein synthesis.

The eIF-4F proteins are perhaps the most specifically targeted of the mRNA-binding initiation factors, yet little is known about their structure or the structural basis for recognition of the cap. The cDNAs of these proteins have been cloned and sequenced from a variety of species (reviewed in Rhoads, 1993). These proteins do not show sequence homology to any other class of proteins in the Brookhaven protein data bank. One must rely on techniques other than x-ray since no crystals have been obtained. Structural information will give more insight into the mechanism of binding and functional properties of the initiation factors. A number of tryptophan residues have been implicated in the binding (Ueda *et al.*, 1991a, b) and an earlier circular dichroism study (McCubbin *et al.*, 1989) of yeast eIF-4E indicated a high β-sheet content. Previous studies (Carberry *et al.*, 1991a) have shown a sharp pH optimum for the binding, possibly due to ionization of a histidine residue. Previously characterized RNA-binding motifs have been identified in other eIFs (McCarthy *et al.*, 1995), although the functional significance of these motifs has yet to be determined.

Circular Dichroism (CD) and fluorescence spectroscopy are powerful tools for spectral analysis of protein structure when x-ray crystallographic data are not available. To understand better the mechanism of protein synthesis initiation, we have used a variety of spectroscopic techniques to obtain structural information and correlate this information with functional properties of the protein. We have examined the conformation of eIF-4F and eIF-(iso)4F and binding with mRNA cap analogs to the initiation factors by employing CD and fluorescence spectroscopy (described in detail in Chapter 4 & 5).

Chapter 2

Mechanisms and Methods

2.1 Fluorescence Steady-state Analysis (Eadie-Hofstee Plot)

The fluorescence titration data (in Chapter 5) were treated according to the following mechanism, which is a simple equilibrium between protein and RNA in a one-to-one stoichiometric ratio. The more complicated data analysis developed by Bujalowski *et al.* (1986 and 1987) with multiple binding sites is not necessary for this system.

For a simple enzymatic reaction scheme:

$$E+S \underset{k_{-1}}{\overset{k_1}{\rightleftharpoons}} ES \qquad (1.1.1)$$

This step involves the reversible binding of enzyme to the substrate to form a complex, ES. Equation 1.1.2 and 1.1.3 can be derived from the above:

$$\frac{d[ES]}{dt} = 0 = k_1[E][S]-k_{-1}[ES] \qquad (1.1.2)$$

and

$$k_1[E][S] = k_{-1}[ES] \qquad (1.1.3)$$

The free enzyme concentration, [E], and the total enzyme concentration, [Eo] are related by

$$[E]=[E_o]-[ES] \qquad (1.1.4)$$

Substituting equation 1.1.4 into equation 1.1.3 gives

$$k_1([Eo]-[ES])[S] = k_{-1}[ES] \quad (1.1.5)$$

$$k_1[Eo][S]-k_1[ES][S] = k_{-1}[ES] \quad (1.1.6)$$

$$k_1[Eo][S] = [ES](k_1[S] + k_{-1}) \quad (1.1.7)$$

$$[ES]=\frac{[Eo][S]}{\frac{k_{-1}+k_2}{k_1}+[S]} \quad (1.1.8)$$

The association constant is defined as $K_{eq}=\frac{k_1}{k_{-1}}$

$$[ES]=[Eo]-\frac{1}{K_{eq}}\bullet\frac{[ES]}{[S]} \quad (1.1.9)$$

K_{eq} can be calculated from the slope of a plot of [ES] versus [ES]/[S]. But this equation cannot be used directly in fluorescence measurements since [ES] is not known. However, because [ES] is directly proportional to the change in the fluorescence signal being observed, we have

$$\Delta F=\Delta F_{max}-\frac{1}{K_{eq}}\bullet\frac{\Delta F}{[S]} \quad (1.1.10)$$

A plot of ΔF against $\Delta F/[S]$ gives a slope of $-\frac{1}{K_{eq}}$, which is the equivalent Eadie-Hofstee plot for treatment of fluorescence quenching data, and is used throughout the thesis.

2.2 Stopped-flow Kinetics

Since the fluorescence of eIF-4F, eIF-(iso)4F and p28 decrease with time upon rapid mixing with m^7GpppG, the elementary steps involved in these interactions were evaluated by stopped-flow spectrofluorimetry. The observed rate constant, k_{obs}, for the change in fluorescence is related in a concentration-dependent manner on the type of basic step to which the relaxation belongs. Two most likely possibilities for protein-ligand interactions, devoid of covalent transformation of either the components, are listed below (Gupta *et al.*, 1992).

For a simple, single bimolecular association between the ligand [C] and the protein [P] (Mechanism (i)), the observed first order change in fluorescence is related to the association and dissociation rate constants and the excess component [C] by Equation (1.2.1), where k_1 and k_{-1} are forward and reverse rate constants, and P and C refer to protein and cap analog, respectively.

$$P + C \underset{k_{-1}}{\overset{k_1}{\rightleftharpoons}} P{\cdot}C \qquad \text{(i)}$$

$$k_{obs} = k_{-1} + k_1[C] \qquad (1.2.1)$$

The second probability involves the rapid formation of an intermediate, (PC)* which isomerizes to yield the final complex PC.

$$P + C \underset{k_{-1}}{\overset{k_1}{\rightleftharpoons}} (P{\cdot}C)^* \underset{k_{-2}}{\overset{k_2}{\rightleftharpoons}} P{\cdot}C \qquad \text{(ii)}$$

which involves a fast association of protein and cap analog followed by a slow change of conformation of the first association complex, (P·C)*, to the stable complex, P·C, giving rise to the fluorescence change. Such a situation k_{obs} is related to various rate constants and [C] by

$$k_{obs}=k_{-2} + k_2\frac{[C]}{K_{-1}+[C]} \qquad (1.2.2)$$

Mechanism (ii) can be written as (Olsen *et al.*, 1993):

$$k_{obs} = \frac{k_2}{1+\frac{K_1}{[C]}} + k_{-2} \qquad (1.2.3)$$

where $K_1 = \frac{k_{-1}}{k_1}$

Equation (1.2.3) can be rearranged to:

$$k_{obs} - k_{-2} = \frac{k_2[C]}{[C]+K_1} \qquad (1.2.4)$$

Under the assumption of $k_{-2} << k_{obs}$, then

$$k_{obs} = \frac{k_2[C]}{[C]+K_1} \qquad (1.2.5)$$

$$\text{and } \frac{1}{k_{obs}} = \frac{1}{k_2} + \frac{K_1}{k_2[C]} \qquad (1.2.6)$$

$\frac{1}{k_2}$ can be obtained from a plot of $\frac{1}{k_{obs}}$ vs $\frac{1}{[C]}$.

Since k_{obs} depends in a characteristic manner on [C], it could be exploited to discriminate experimentally between these two mechanisms outlined above. From Equation (1.2.1), it follows that k_{obs} would increase linearly with [C]; while Equation (1.2.5) predicts that k_{obs} would increase linearly with [C] but would tend to saturate as [C] increases from a value much lower than $1/K_1$ to [C] $>>1/K_1$.

2.3 Protein Purification

The protein synthesis initiation factors eIF-4F and eIF-(iso)4F studied in this thesis were isolated according to the procedure described in Lax *et al.* (1986a, b), Browning *et al.* (1987) and Carberry *et al.* (1991b). The key steps include buffer E (20 mM HEPES-KOH, pH 7.6, 1 mM $(CH_3COO)_2Mg$, 2 mM $CaCl_2$, 6 mM BME, 120 mM KCl, 0.1 mg/mL of STI, and 0.5 mM PMSF) extraction, ammonium sulfate precipitation, DE-52 column separation, m^7GTP column purification and buffer B(120) dialysis. Buffer B consisted of 20 mM HEPES-KOH, pH 7.6, 0.1 mM EDTA, 1 mM DTT, 10% glycerol, and KCl as indicated by its molar concentration.

2.3.1 Buffer E Extraction

The way to start purifying eIF-4F and eIF-(iso)4F was the same. All the procedures were carried out at 0-4°C unless indicated otherwise. 200 grams of wheat germ were reduced to a fine powder by grinding in a Waring blender followed by mixing with 340 ml Buffer E (20 mM HEPES-KOH, pH 7.6, 1 mM $(CH_3COO)_2Mg$, 2 mM $CaCl_2$, 6 mM BME, 120 mM KCl, 0.1 mg/ml of STI, and 0.5 mM PMSF) and centrifuging at 15,000g for 20 minutes. The supernatant was loaded onto a Sephadex G-25 column.

The effluent coming from the column, 450 ml or so, was centrifuged at 30,000 g for 20 minutes. The resultant final supernatant, called 120 mM KCl wheat germ extract supernatant, was stored in a -150°C freezer before being used for the next step.

2.3.2 Ammonium Sulfate Precipitation

The entire 120 mM KCl supernatant from above was thawed slowly at 4°C. Finely powdered ammonium sulfate (24.3mg/100ml) was gradually added to the solution to 40% saturation. After stirring for 30 minutes, the cloudy solution was centrifuged for 20 minutes at 15,000 g (approximate 12,500 rpm for Sorvall). The pellets were resuspended in small amount of buffer B-40 (40 mM KCl), and dialyzed against B-40 overnight at 4 °C.

2.3.3 DE-52 Column Separation

The B-40 dialyzed fraction from the 40% ammonium sulfate precipitation was loaded onto a DE-52 column (detailed in Sha Ph.D. thesis, pp20-24), equilibrated with buffer B-40. The column was washed until the absorbance at 280 nm was below 0.2 to remove all the non-bound proteins. The buffer was changed to B-80 (80 mM KCl)

then, and the one major peak containing eIF-(iso)4F and eIF-4B was collected. The column was washed by B-80 after collection until the absorbance returned to the baseline. The buffer was changed to B-120 (120 mM KCl), and the peak containing eIF-4F was collected. Both DE-52 peak fractions were precipitated with 80% ammonium sulfate (51.6 g/100 mL), centrifuged at 11000 rpm in a Sorvall centrifuge; the precipitate, which contained eIF-4F or eIF-(iso)4F and eIF-4B, were resuspended in approximately 10 mL of B-120 and dialyzed overnight against B-120.

2.3.4 m^7GTP Column Purification

This step was used to separate eIF-(iso)4F which was bound to m^7GTP column and eIF-4B which was flow-through and to purify eIF-4F since it is also a m^7GTP cap binding protein. The dialyzed samples were applied to 1 mL m^7GTP-Sepharose column equilibrated in B-120 (detailed in Sha, Ph.D. thesis, pp25-31). The columns were washed with 20 mL B-120 and the proteins were eluted by B-120 containing 10 mL 70 μM m^7GTP. In order to maximize yields, the m^7GTP solution was freshly prepared and the sample was poured into the column 5 ml each twice.

2.3.5 Buffer B(120) Dialysis

The proteins prepared in this manner contain m^7GTP. It is necessary to remove m^7GTP from the solution. After dialyzed against B-120 for 4 hours with stirring, the samples were pooled into 10% PEG in B-120 solution to remove m^7GTP further and concentrated down to 0.5 ml. The purities were checked on a 7% SDS denaturing mini-gel electrophoresis with 4% stacking gel. Two bands of p86 and p28 and two bands of p220 and p26, as the large and small subunits of eIF-(iso)4F and eIF-4F, respectively, were observed.

Chapter 3

Instrumentation

3.1 Circular Dichroism

X-ray crystallography is often used to determine the three dimensional crystal structure of protein, but it is expensive, laborious, and time-consuming, often requiring months or even years for a single protein. What is more, many proteins are notoriously difficult to crystallize. Nuclear magnetic resonance (NMR) spectrometry can be used to determine the structure of proteins in solution, but the method is currently limited to smaller proteins. In contrast, circular dichroism can be applied to estimate the secondary structure of proteins.

Most biological molecules contain a number of electronic units that absorb light nearly independently, called chromophores, that are asymmetrically disposed in space. Such asymmetric molecules will absorb left circularly polarized light differently from right circularly polarized light. Circular dichroism (CD) is the difference in absorption between left and right circularly polarized light, so that CD spectral bands occur wherever there are normal electronic absorption bands in an asymmetric molecule. The CD is generally measured by passing alternately right- and left-handed circularly polarized light through the sample and measuring the difference in their optical transmission. After passing through an optically active absorbing sample, the light is changed in two aspects. The maximal amplitude of the electric vector traces out an ellipse. The arc tangent of the ratio of the minor axis to the major axis is called

ellipticity. The orientation of the ellipse is changed. In the literature, CD spectra are reported in units of $\Delta\varepsilon$, $\Delta\varepsilon = \varepsilon_l - \varepsilon_r$, where $\Delta\varepsilon$ is the difference in extinction coefficient between left-handed ε_l and right-handed beams ε_r. The ellipticity of light, θ, is the ratio of the minor to the major axis of the ellipse. It is related to $\Delta\varepsilon$ by

$$\theta \text{ (radians)} = (2.303cl/4)\,\Delta\varepsilon$$

where the concentration c is in moles per liter and l is the pathlength in centimeters. CD spectra are also expressed in units of molar ellipticity, $[\theta]$ in degrees per decimeter,

$$[\theta] = \theta \text{ (radians)}\,(180/\pi)\,100/cl$$

As one can see from the above, $[\theta]$ and $\Delta\varepsilon$ are simply proportional by

$$[\theta] = 3300\Delta\varepsilon$$

The CD of proteins is primarily the CD of the amide chromophore: secondary structure as measured by CD counts amide-amide interactions, a somewhat different number from counting residues in X-ray diffraction structures. CD spectra are influenced by concentrations, solvent and other factors. At high concentration, protein itself may fold in a certain way that causes the changes of $\Delta\varepsilon$. CD signal does not relate to the concentration in a linear manner all the time.

A schematic diagram of Jasco J-710, the instrument used for CD measurement in this study, is shown on the next page.

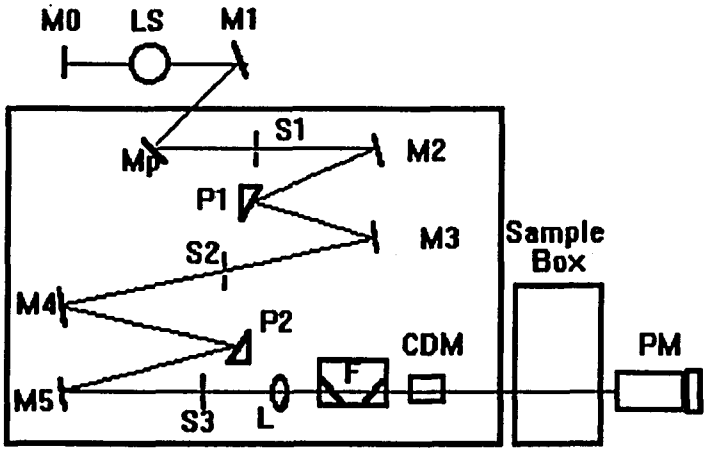

Figure 3.1. Schematic diagram of the J-710 Jasco CD Spectropolarimeter. From J-710 Spectropolarimeter Instruction Manual.

M0, M1, Mp, M2, M4, M5 : Mirrors

LS : Light source

S1, S2, S3 : Slits

P1 : First prism (horizontal optical axis)

P2 : Second prism (vertical optical axis)

L : Lens

F : Filter

CDM : CD modulator

PM : Photomultiplier tube

The xenon lamp is used as the light source. The light from the light source is focused by the mirror M1 onto the entrance slit S1. The first monochromator and second monochromators refer to the optical system between S1 and the intermediate slit S2, and that between the intermediate slit S2 and the exit slit S3, respectively. The prisms P1 and P2 having different axial directions, so that the light passing through the monochromator is not only monochromated but also linearly polarized, oscillating in the horizontal direction. This linearly polarized light is modulated by the CD modulator to the right and left circularly polarized beams of light. The CD modulator is an element that subjects quartz to mechanical stress to produce circular polarization in the crystal.

3.2 Fluorescence

Substances which display significant fluorescence generally possess delocalized electrons formally present in conjugated double bonds. Proteins contain three amino acid residues which may contribute to their ultraviolet fluorescence: tyrosine, tryptophan, and phenylalanine where the emission occur due to $\pi^* \rightarrow \pi$ transition. The characteristic excitation and emission maxima of these three amino acid residues are shown in Table 3.1. For the fluorescence studies of eIF-4F and p26, eIF-(iso)4F in this thesis, 290 nm and 340 nm are used as the absorption and emission wavelengths. It can be seen that the fluorescence of the proteins is dominated by the tryptophan residues.

Amino Acid	Excitation Maxima (nm)	Emission Maxima (nm)
phenylalanine	255	280
tyrosine	280	300
tryptophan	280	340

The excitation of fluorescence is brought about by absorption of photons. Fluorescence can occur in simple as well as in complex gaseous, liquid, and solid chemical systems. When one of a pair of electrons of a molecule is excited to a higher

energy level, a singlet or a triplet is permitted. Fluorescence and phosphorescence are the emissions of photons from electronically singlet and triplet excited states to the ground states, respectively. The properties of a molecule in the excited triplet state differ significantly from those of the excited singlet state. A singlet/triplet transition, which involves a change in electronic state, is a significantly less probable event than the corresponding singlet/singlet transition.

An excited molecule can return to its ground state by a combination of several mechanistic steps. Two of these steps, fluorescence and phosphorescence, involve the release of a photon of radiation. Other deactivation steps are radiationless processes which include vibrational relaxation, internal conversion, external conversion, and intersystem crossing. The quantum yield for fluorescence or phosphorescence is simply the ratio of the number of molecules that luminesce to the total number of excited molecules. An electronically excited molecule normally returns to its lowest excited state by a series of rapid vibrational relaxation and internal conversions that produce no emission of radiation. Thus fluorescence most commonly arises from a transition from the first excited electronic state to one of the vibrational levels of the electronic ground state.

The fluorescence spectra were measured on SPEX Fluorolog-τ2 spectrofluorimeter (Figure 3.2), which includes six main parts: lamp, excitation monochromator,

modulator compartment, sample compartment and detector-emission monochromator. The sample beam first passes through an excitation monochromator, which transmits radiation that will excite fluorescence but excludes or limits the emitted radiation. Fluorescence is observed at right angles to the excitation beam; at other angles, increased scattering from the solution and the cell walls may cause large errors in the measurement of intensity. The emitted radiation reaches the detector after passing through the emission monochromator. The fluorescence intensity *vs.* wavelength was recorded and processed on a Gateway 2000 computer.

Figure 3.2. Schematic diagram of the Fluorolog-τ2 spectrofluorimeter.

From SPEX Fluorolog-τ2 Operation Manual 4-7.

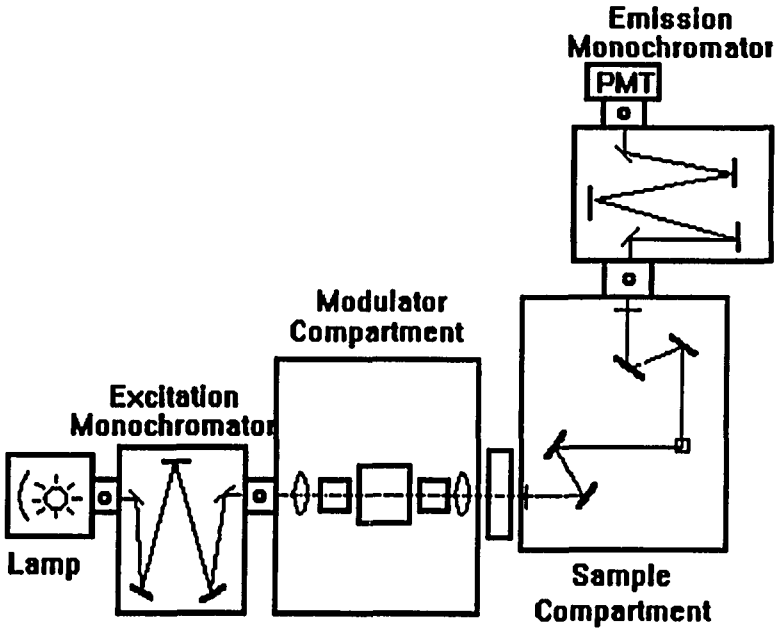

3.3 Stopped-flow Kinetics

In order to measure the rate constants of individual steps on the reaction pathway and detect transient intermediates, it is necessary to measure the rate of approach to the steady state. The most popular techniques for the measurement of the rate constant for a reaction in solution involves the mixing of reagent solutions followed by spectrophotometric monitoring of the reaction mixture. Three types of techniques have been utilized for this purpose (Fersht, A., 1984): rapid mixing and sampling, flash proteolysis and relaxation methods. The stopped-flow method is an extremely useful rapid mixing technique since it is possible to mix two solutions in a fraction of a millisecond, and the majority of enzyme turnover numbers are less than 1000 s^{-1} . In this work, the kinetics of the interaction between p28, eIF-(iso)4F (Chapter 4) and eIF-4F (Chapter 5) with cap analogs were monitored by a Hi-Tech Scientific SFA-11 stopped-flow apparatus.

The Hi-Tech Scientific SFA-11 Fast Kinetics Accessory (shown in Figure 3.3) is composed of a drive unit, thermostatted supply tube and an observation cell with integral mixer. The flow circuit is made of glass and Teflon and the observation cell is of fused silica. The cell is of special design with a two-jet mixer with 2x10mm pathlengths. Temperature can be measured by inserting a thermometer at point A,

indicated in the diagram. The use of the spectrophotometer's thermostatted cell holder and an external thermostatted circulator will provide close temperature control.

Figure3.3. Apparatus of the Stopped-flow spectrofluorimeter. Redraw from SFA-11 Rapid Kinetics Accessory Manual.

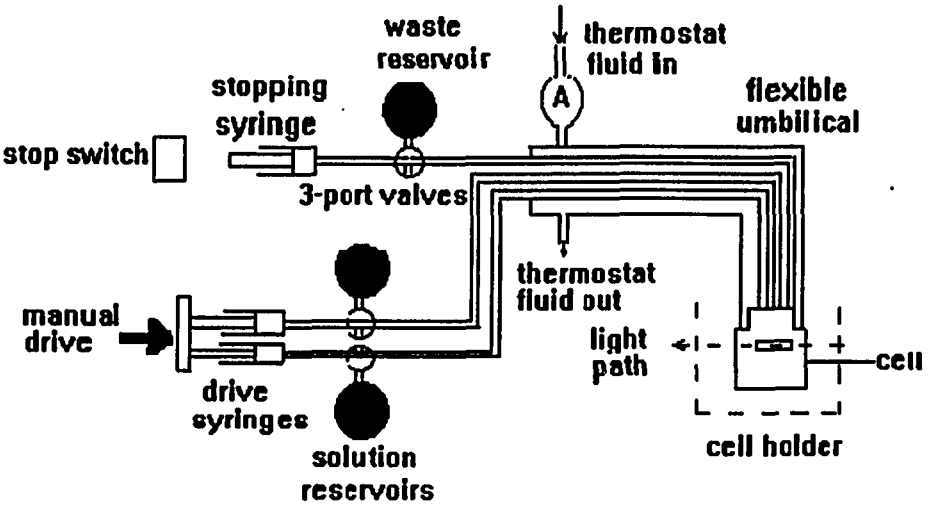

Chapter 4

pH-Dependent and Ligand Induced Conformational Changes of Eukaryotic Protein Synthesis Initiation Factors eIF-(iso)4F: Circular Dichroism and Stopped-flow Kinetic Studies

In higher plants, eIF-4F exists in an isozyme form (eIF-(iso)4F) (Lax *et al.*, 1985; & Browning *et al.*, 1987 & 1992). This isozyme form has not been identified in any other eukaryotes. The isozyme form of eIF-4F contains two subunits, p86 and a m^7G cap-binding protein, p28 (Browning *et al.*, 1987). The functional properties of eIF-(iso)4F are similar to those of eIF-4F from wheat in : (1) supporting polypeptide synthesis in an *in vitro* translation system deficient in eIF-4F; (2) binding of mRNA to 40S ribosomal subunits; and (3) hydrolyzing ATP in the presence of eIF-4A, eIF-4B and mRNA (Lax *et al.*, 1985 & Browning *et al.*, 1987). Recently, van Heerden and Browning (1994) expressed the individual subunits, p86 and p28, in *E. coli* and showed that the individual subunits alone were not able to support polypeptide synthesis. However, when the subunits were recombined at a 1:1 molar ratio, their activity was equal to that of the native form.

eIF-(iso)4F can substitute for its isozyme form, eIF-4F, in catalyzing RNA-dependent hydrolysis of ATP in the presence of mammalian eIF-4A and in promoting the cross-linking of mammalian eIF-4A to the 5'-terminal cap of oxidized mRNA (Abramson *et al.*, 1988). Carberry *et al.* (1991b) showed by direct fluorescence measurement that eIF-(iso)4F behaved differently from other cap binding proteins in terms of their ability to bind m^7GTP and other mRNA analogs. Those results suggested that eIF-4F and eIF-(iso)4F factors may have discriminatory or regulatory roles in selecting mRNA for translation in higher plants.

Here, CD spectroscopy was used to assess the types and amounts of secondary structural features of eIF-(iso)4F and eIF-4F under different pH conditions. In addition, the availability of the expressed individual subunits, p86 and p28, allowed conformational studies of the individual subunits and recombinant complex of eIF-(iso)4F from wheat germ.

4.1 Experimental Procedure

4.1.1 Materials

eIF-(iso)4F was isolated from wheat germ as described by Carberry *et al.* (1991a). A molecular weight of 108,000 was used to calculate the molar concentration. The two subunits p28 and p86 were purified from *E. coli* extracts containing the expressed proteins as previously described (van Heerden & Browning, 1994). m^7GTP and m^7GpppG were purchased from Pharmacia Molecular Biologicals. Potato acid phosphatase (5.3 unit/mg) was from Sigma. The Microcon 3 concentrator was obtained from Amicon.

The 5' capped oligoribonucleotides were prepared by cell-free transcription in a T7 RNA polymerase system as described elsewhere (Carberry *et al.*, 1992). The

phosphatase treatment of eIF-(iso)4F was similar to that of eIF-4E (Minich *et al.*, 1994). eIF-(iso)4F 0.3 μM was incubated with potato phosphatase (7 unit/ml) in 50 mM Pipes, 1 mM DTT, 10% glycerol, pH 5.8 for 2.5 hrs at room temperature. The phosphatase was removed by chromatography on m^7GTP-Sepharose column. The bound protein was eluted with 75 μM m^7GTP in buffer A, which consisted of 20 mM HEPES-KOH, 0.1 mM EDTA, 1 mM DTT, 10% glycerol, and 120 mM KCl. The cap analog was removed by using Microcon 3 concentrators with at least three times dilution of buffer A.

4.1.2 CD Measurements

CD spectra were measured on a Jasco-J710 spectropolarimeter. Spectra of eIF-(iso)4F were obtained in buffer A, which consisted of 20 mM HEPES-KOH, 0.1 mM EDTA, 1mM DTT, 10% glycerol, and 120 mM KCl. Spectra of p28 and p86 were measured in buffer B, 20 mM HEPES-KOH, 0.1 mM EDTA, 10% glycerol, and 100 mM KCl, pH 7.6.

All spectra were obtained with 0.5 mm pathlength quartz cell at ambient temperature. The instrument was routinely calibrated with ammonium d-(+)-10-camphor sulfate according to the procedures outlined by the manufacturer. Each sample was scanned 40 times and high frequency noise reduction applied before calculating mean residue

ellipticities. Data were recorded at 0.5 nm intervals with a time constant of 1.0 s and 1.0 nm constant spectral bandwidth. The mean residue ellipticity, [θ], was calculated by using a mean residue weight of 115.0 and expressed in $degcm^2dmol^{-1}$.

4.1.3 Computer-Assisted Analysis

The secondary structure of eIF-(iso)4F and its two subunits have been estimated using the SELCON program, developed by Sreerama and Woody (1993), which analyses CD spectra as a sum of data collected from 17 proteins whose structures are known from x-ray crystallography based on self-consistent method. Secondary structures were also estimated from the amino acid sequence by the predictive methods of Chou and Fasman (1978), and Garnier *et al.* (1978) applied to p28 and p86.

A composite surface profile was drawn showing the regions of sequence most likely to lie on the surface of the protein, and their hydrophilicity. This computer-generated profile is a composite of four approaches which include surface probability, hydrophilicity, antigenicity (data not shown) and flexibility (data not shown). The sequence was analyzed on the GCG sequence analysis software package programmed by the University of Wisconsin-Madison.

4.1.4 Stopped-flow Kinetics

Stopped-flow fluorescence experiments were performed on a Hi-Tech SF-51 stopped-flow spectrofluorometer equipped with a Berger-type mixing chamber and a 2x2x10 mm flow cell with a dead time ~1.5 ms. The excitation wavelength was 280 nm, slit width 2 mm. Light emitted from the reaction mixture was monitored after passage through a cut-off emission filter (WG-320 provided by Hi-Tech). A series of stopped-flow experiments was carried out at 23^{o}C in buffer A, pH 7.05 under different concentrations of cap analogue m^{7}GpppG. After rapid mixing of the protein with the mRNA cap, the time course of the intrinsic fluorescence intensity was recorded.

4.2 Results and Discussion

Circular dichroism measurements in the far UV region yield data that may be equated with the general secondary folding of the protein molecule, i. e. amount of α-helix, β-sheet, β-turn, or random coil. In this study, we measured the CD spectra from 185 to 300 nm of the intact eIF-(iso)4F itself and the interaction with cap analogs under different pH conditions. The two subunits p28 and p86 of eIF-(iso)4F plus their complex were measured at pH 7.6 to establish the secondary structures of these proteins and any conformational changes that might result due to changes in pH and binding of cap analogs.

Far UV CD data for eIF-(iso)4F are presented in Fig. 4.1. At pHs other than 7.6, the spectra of the native protein are characterized by minima at 208 and 222 nm, representing the formation of an α-helical conformation. In the more acidic condition (pH < 7.6), the ellipticity at 222 nm increases from -4800 to -3500 $degcm^2dmol^{-1}$. In the more basic condition (pH > 7.6), the ellipticity at 222 nm decreases from -3300 at pH 8.0 to -4500 $degcm^2dmol^{-1}$ at pH 8.6. One of the characteristics of the presence of the substantial fraction of α -helix is the presence of the minima at 208 and 222 nm. The flattening of the spectrum between the nearly equivalent minima at 208 and 222 nm is a characteristic feature found in proteins of the α/β structural class that contain

domains comprised of intermixed α-helical and β-sheet structures (Brahms & Brahms, 1980; & Manavalan & Johnson., 1983). At pH 7.6, which is the optimum cap binding condition, the spectrum lacks minima at 208 or 222 nm, indicating that the structural elements present in the native protein have adopted conformations other than the dominant α-helix.

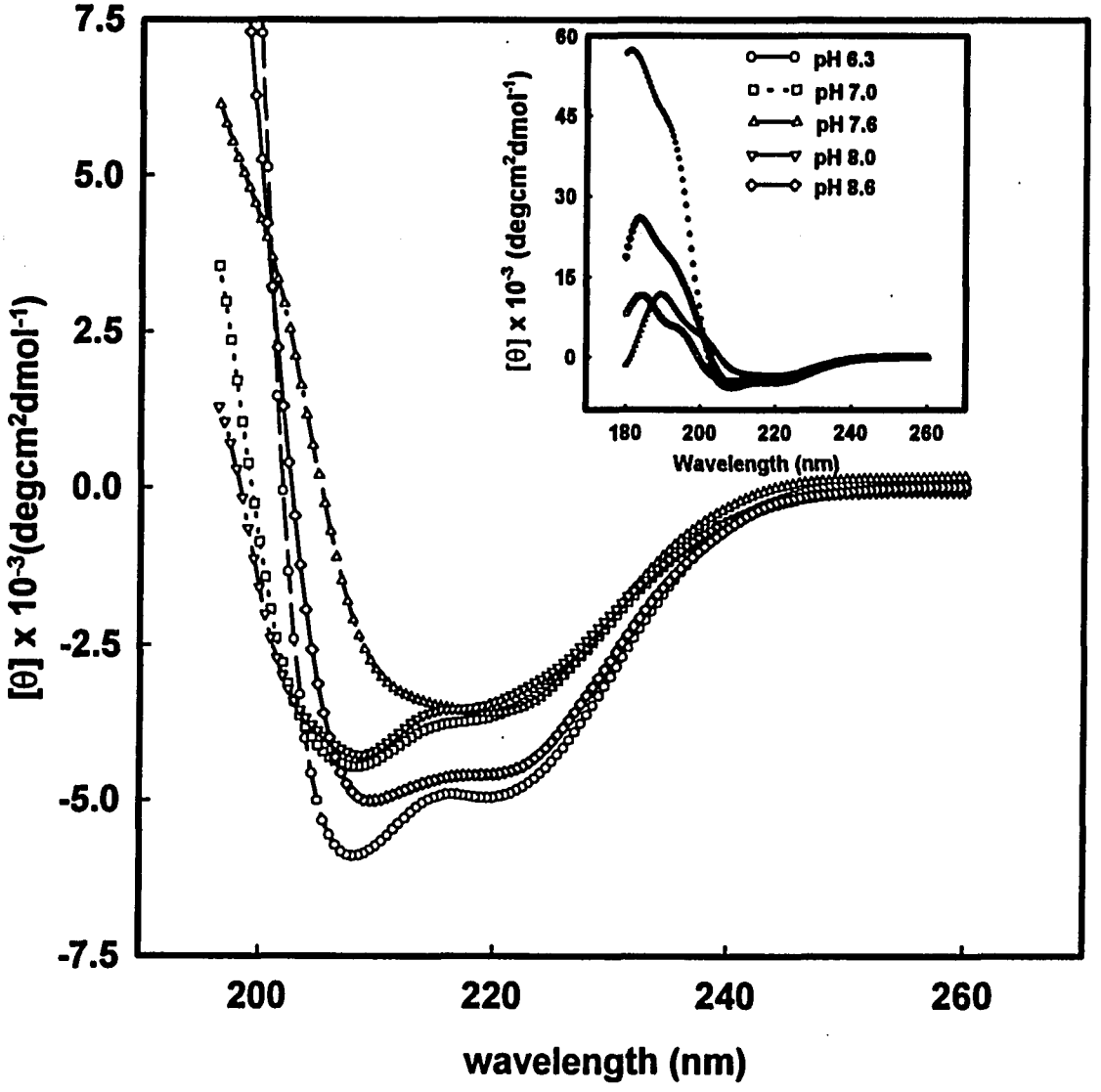

Figure 4.1. CD spectra of eIF-(iso)4F as a function of pH. The solvent system was 20 mM HEPES-KOH, 0.1 mM EDTA, 1 mM DTT, 10% glycerol, and 120 mM KCl. The concentration of eIF-(iso)4F was 0.186 mg/mL. **Inset:** spectra were drawn from 180 to 260 nm.

The far UV CD spectra were analyzed by the method of Sreerama and Woody (1993) to estimate the abundance of secondary structural elements within eIF-(iso)4F. The results are shown in Table 4.1. At pH 6.3 and 8.6 (Fig. 4.1), the α-helix was the predominant secondary structural element within eIF-(iso)4F, comprising about 40% of the total. At pH 7.6, the native protein has a lowest α-helical content (≈15%), the major structural features being β-sheet (some 38%) and β-turns (about 22%). While determining the exact % of each of these structural elements by CD is not possible, these estimates are generally accurate to about ±5%.

The negative charges of the RNA phosphate residues must serve to destabilize the α-helix, unlike small anions (Goto & Amito, 1991). RNA-binding studies indicate that β-sheet possibly is one of the distinct structural elements of an RNA-binding domain and probably is in contact with RNA. An RNA-binding domain is present in one or more copies in proteins that bind pre-mRNA, mRNA, pre-ribosomal RNA, and small nuclear RNAs (Burd & Dreyfuss, 1994). This implies that if eIF-(iso)4F has a β-sheet binding domain, that pH 7.6, at which it has the richest β-sheet content, would be the optimal condition for cap binding. This conclusion agrees with our previous binding studies (Carberry *et al.*, 1991a).

The CD spectra were also measured for the two subunits p28 and p86 at pH 7.6. Both subunits contain a substantial fraction of α-helix. p28 has a somewhat higher amount of α-helix than p86, 60% *versus* 34% (Table 4.2). The combination of these two subunits cause some secondary structure changes, *i.e.*, less α-helix, more β-sheet, etc. It was noticed that there were some conformational differences in the native complex and recombinant complex (Fig. 4.2 & Table 4.2). The recombinant complex has the same activity in *in vitro* translation assays as the native complex (van Heerden & Browning, 1994). To determine if there was some difference in the method of preparing the complex, the samples used for the CD spectra were also tested for activity and found to be identical (data not shown). These results suggest that the differences in folding do not appear to affect the activity, at least *in vitro*. However, it is possible that other factors (*e. g.*, eIF-4A, eIF-4B, phosphorylation *etc.*) are causing conformational changes in the recombinant protein during the polymerization assay, that allow the recombinant protein to fold properly. To test this hypothesis, the subunits were incubated in the presence of eIF-4A, eIF-4B, eIF-3, mRNA and ATP and the complex (p28 + p86) was isolated on a m^7GTP Sepharose column. A second possibility is that post-translational modifications, such as phosphorylation affect the protein conformation. To test this possibility, native eIF-(iso)4F was treated with potato acid phosphatase that caused the dephosphorylation of eIF-(iso)4F. The CD spectra and analysis of the "pretreated" complex, a control that was incubated only in the presence of mRNA and ATP prior to isolation on m^7GTP Sepharose, untreated

recombinant complex and the dephosphorylated form are shown in Table 4.2 and Fig.4.2. The "pretreated" sample incubated with other initiation factors and the "control" incubated with mRNA and ATP are essentially identical. These samples are still different from the native protein. However, the phosphatase treatment altered the protein conformation from its native state to a conformation much closer to the "pretreated" form, implying that phosphorylation influenced protein folding.

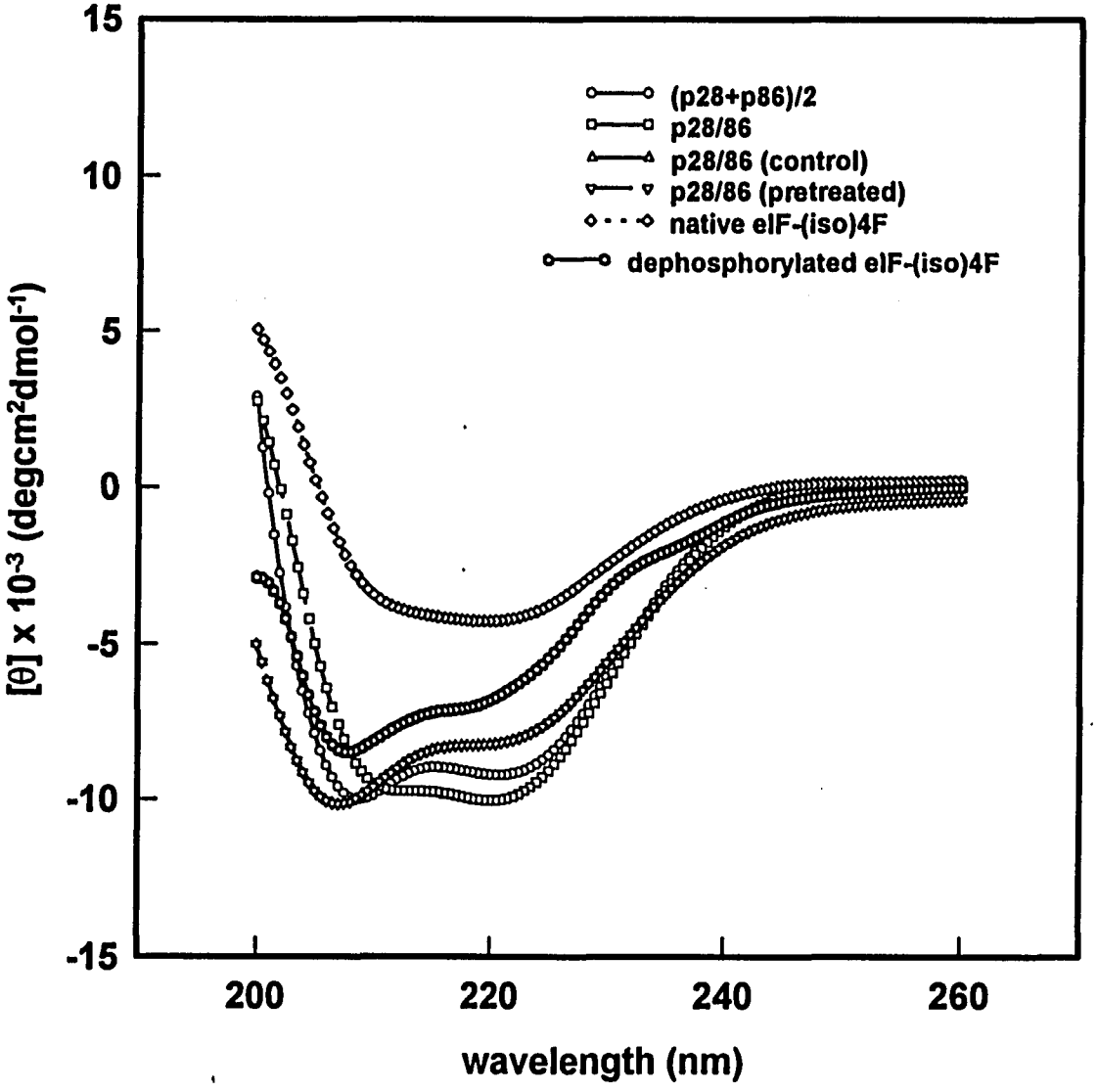

Figure 4.2. Comparison of CD spectra of native wheat germ eIF-(iso)4F and complex of p28 and p86 with 1:1 molar ratio at pH 7.6. The concentrations of p28 and p86 were 0.056 mg/mL and 0.164 mg/mL respectively. The buffer system was the same as in Figure 4.1.

The abundance of secondary structural elements in p28 was compared with those obtained using the methods of Chou and Fasman (1978) and Ganier, Osguthorpe, and Robson (Ganier *et al.*, 1978) analysis from sequence data (Figure 4.3, Allen *et al.*, 1992) through the GCG sequence analysis software package. The compositional results are shown in Table 4.3-a & b and 4.4-a & b. It is apparent from these data that the higher values of α-helical content, coupled with the corresponding lower values for β-sheet, agree closely with the experimentally observed figures.

The pH dependent far-UV CD spectra of eIF-(iso)4F in the absence and presence of several nucleotides (Figure 4.4) are shown in Fig. 4.6 & 4.7 (Fig. 4.6, pH 6.3; Fig. 4.7, pH 7.6). The nucleotides chosen for this study were all methylated at the guanine N-7 position. At pH 6.3 (Fig. 4.6), the addition of 5-fold molar excess of cap analogs leads to dramatic changes in the CD spectrum of the protein. The ellipticities at 208 and 222 nm both become less. Separate experiments had shown that the nucleotides alone, at the concentrations employed here, displayed practically no ellipticity in this wavelength range.

p28 (wheat germ):

1 MAEVEAALPV AATETPEVAA EGDAGAAEAK GPHKLQRQWT

His 33 Trp 39

41 FWYDIQTKPK GPAAWGTSLK KGYTFDTVEE FWCLYDQIFR

Trp 42 Trp 55 Trp 72

81 PSKLVGSADF HLFKAGVEPK WEDPECANGG KWTVISSRKT

His 91 Trp 101 Glu 105 Trp 112

121 NLDTMWLETC MALIGEQFDE SQEICGVVAS VRQRQDKLSL

Trp 126

161 WTKTASNEAV QVDIGKKWKE VIDYNDKMVY SFHDDSRSQK

Trp 161 Trp 178 His 193

201 PSRGGRYTV

Figure 4.3 Amino acid sequence of p28 subunit of wheat germ eIF-(iso)4F. Histidine and tryptophan residues are in bold and labeled by numbers. Numbers are started from N-terminal. Allen *et al.*, 1992.

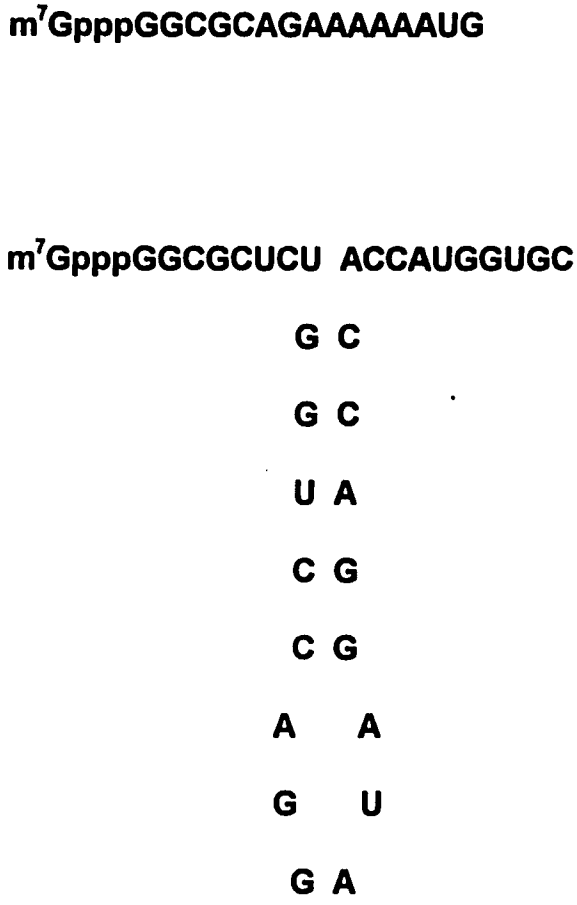

Figure 4.4 Structures of the capped oligonucleotide with and without hairpin.

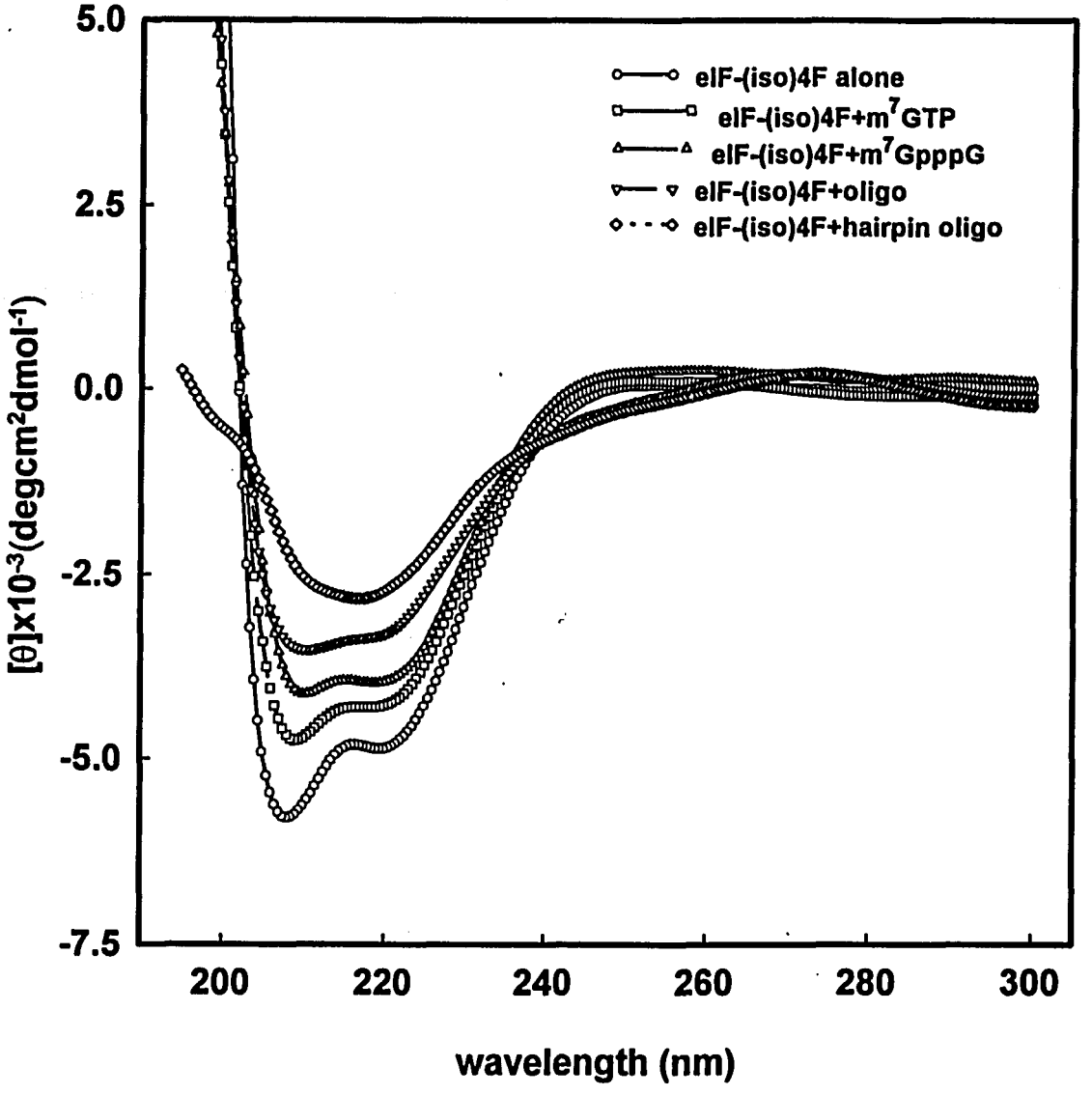

Figure 4.5. Far-UV CD spectra for eIF-(iso)4F at pH 6.3 in 20 mM HEPES-KOH, 0.1 mM EDTA, 1 mM DTT, 10% glycerol, and 120 mM KCl. Protein concentration 0.186 mg/mL, 5- fold molar excess of cap analogs, and 0.05 cm pathlength cell were used.

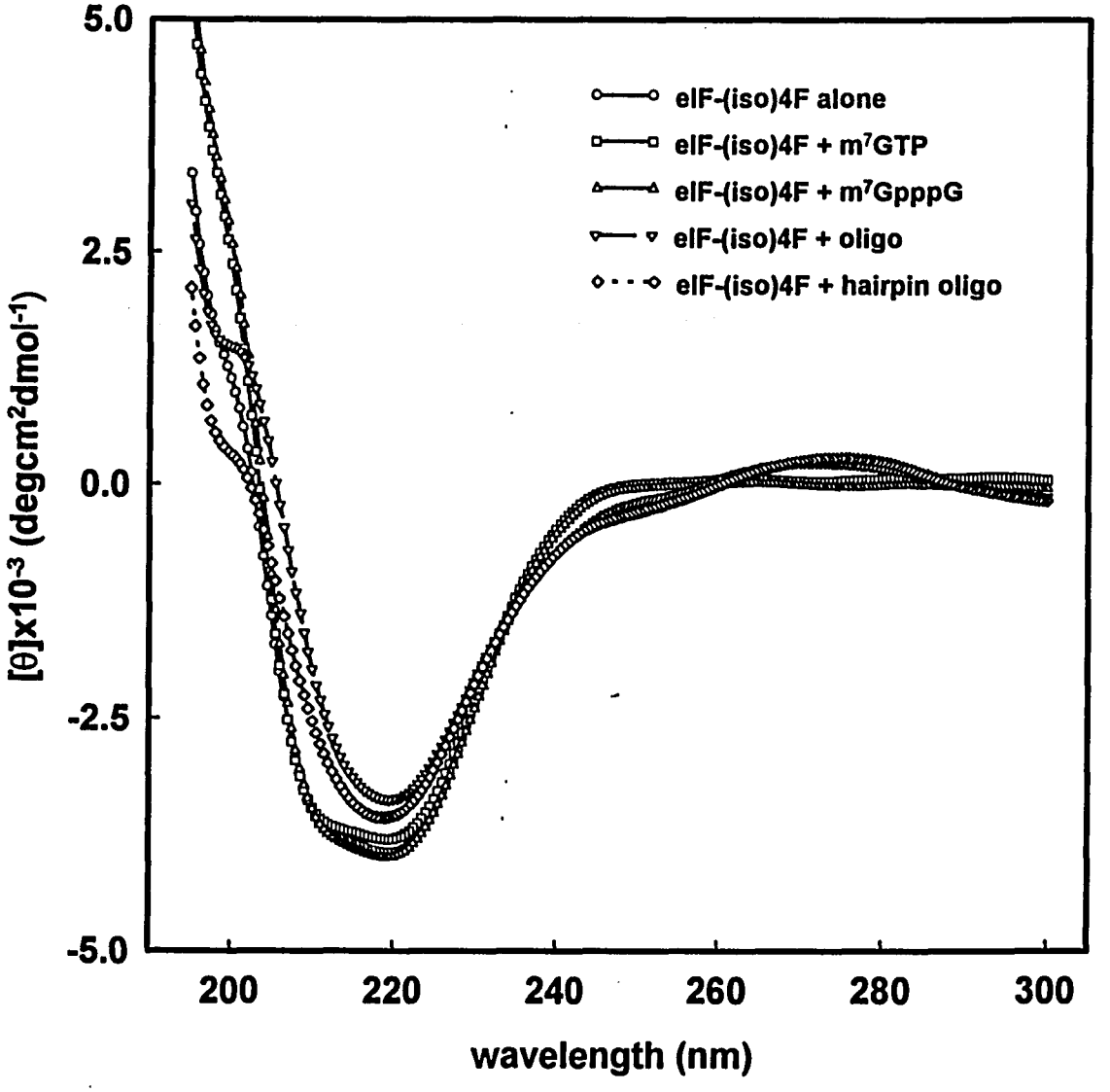

Figure 4.6. Far-UV CD spectra for eIF-(iso)4F at pH 7.6. The experiment conditions were the same as in Figure 4.5.

Analogous experiments were also performed at pH 7.0 (data not shown), 7.6 (Fig.4.6), 8.0 (data not shown) and 8.6 (data not shown). In contrast to the other pHs, at pH 7.6, all the spectra of eIF-(iso)4F are characterized by a minimum near 222 nm. The proportion of α-helical structure in eIF-(iso)4F at pH 6.3 is higher than that found at pH 7.6, which instead is dominated by a rich β-sheet conformation. Upon addition of nucleotides, a reduction in CD signal was noted across the entire wavelength range. These changes ranged from $[\theta]_{220}$ = -3800 degcm^{2}dmol^{-1} for m^{7}GTP to $[\theta]_{220}$= -3400 degcm^{2}dmol^{-1} for the hairpin oligonucleotide. The computer program SELCON was applied to analyze the CD spectra. The results are represented in Table 4.1. It was noticed that m^{7}GpppG reduced the α-helix content by 18%, with an 4% increase in β-sheet at pH 7.6, while it lowered the α-helix content by 69% and elevated β-sheet content by 184% at pH 6.3. The addition of cap analogs, m^{7}GTP and m^{7}GpppG to p28 also caused significant conformational changes (Table 4.2).

The CD spectra of eIF-(iso)4F upon binding of mRNA analogs are dependent on the oligonucleotide used. Previous studies showed that the mRNA with decreased secondary structures are better initiators (Reviewed in Edery *et al.*, 1987). In Fig. 4.5 & 4.6, the small peaks around 275 nm were attributed to the absorption of mRNA cap analogs. The oligonucleotides with greater secondary structure produce more significant changes in the protein conformation than the cap analogs (Table 4.1). This

is in agreement with earlier binding studies which show that capped oligonucleotides bind more efficiently than cap analogs suggesting that other bases adjacent to the cap are in contact with the protein and are involved in binding.

NMR studies have shown that the RNA binding domain within proteins is typically composed of a compact folded structure (βαββαβ) (Reviewed by Burd *et al.*, 1994). Gorlach *et al.* (1992) suggested it is the β-sheet, not α-helices, that constitute the binding domain. This exposed β-sheet binding domain could provide an open platform rather than a buried mode for the RNA contact. It was concluded (Burd *et al.*, 1994) that the structures of the RNA-binding domain proteins in eukaryotic cells when bound to RNA is similar to the unbound structure. If the eIF-(iso)4F binding domain is a β-sheet domain, one should expect the smaller conformational change of eIF-(iso)4F in the presence of cap analogs at pH 7.6 since more β-sheet is present. This is shown in Table 4.1.

One of the surprising aspects of this study is the ability of mRNA analogs to induce a large conformational change at pHs other than the optimal binding pHs. There are 9 tryptophan residues in p28 (Allen *et al.*, 1992). The fluorescence studies of wheat germ eIF-(iso)4F (Carberry *et al.*, 1991a) suggest the involvement of tryptophan and histidine residues in the cap-binding site. We have found the small subunit, p28 binds

cap analogs (Sha *et al.*, 1995) with high affinity. It is interesting to note the positions of the tryptophan and histitine residues in p28 subunit. Utilizing a composite algorithm for surface probability (Emini *et al.*, 1985) and hydrophilicity (Hopp & Woods,1981), a surface profile (Fig. 4.7) could be predicted showing the regions most likely to lie on the surface of the protein.

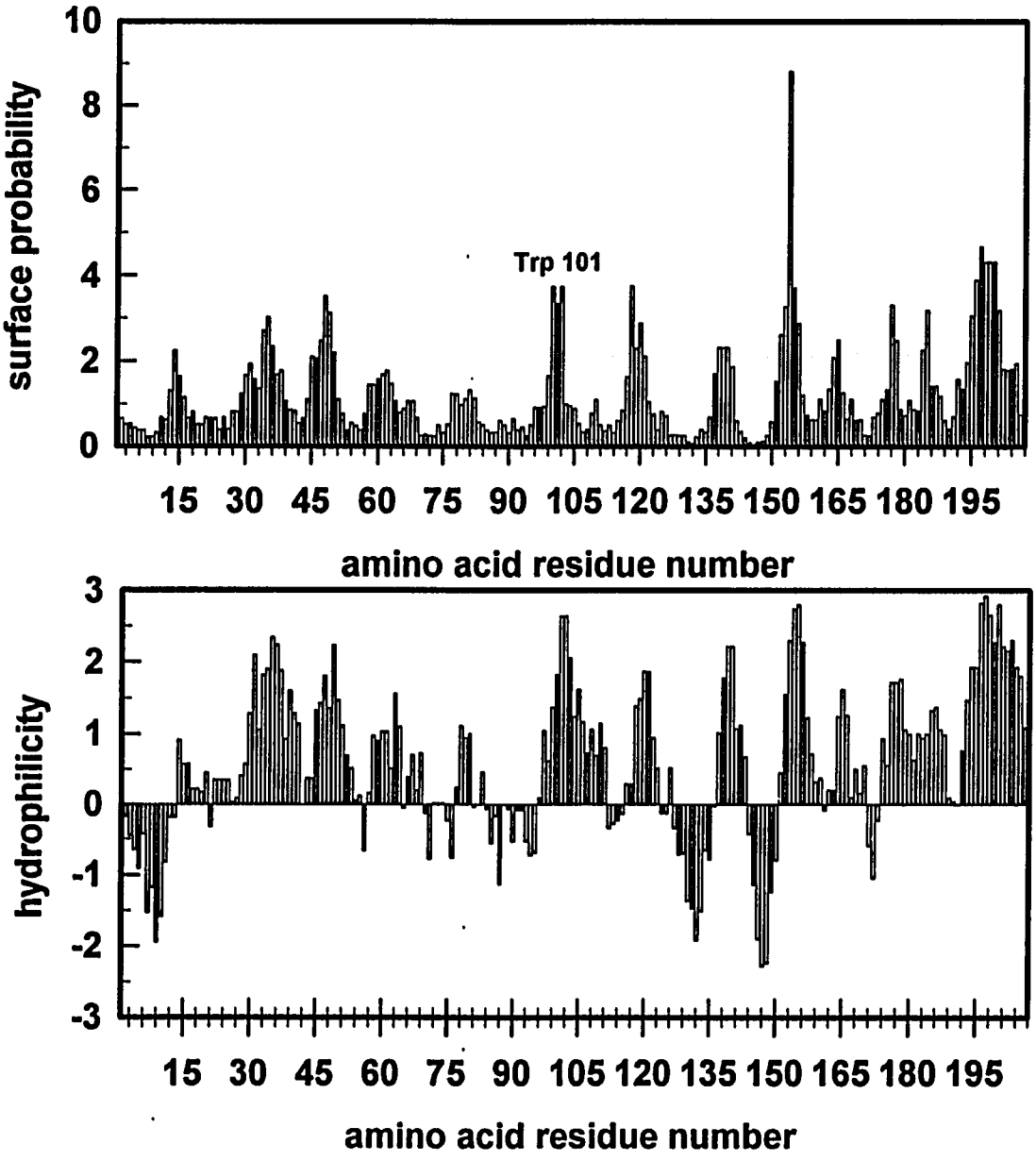

Figure 4.7. Plots of surface probability and hydrophilicity for p28. The PEPTIDE STRUCTURE program (Emini *et al.*, 1985, & Hopp *et al.*, 1981) in GCG package was used.

Ueda *et al.* (1991a,b) proposed that base stacking of the tryptophan and hydrogen-bond pairing by the glutamic acid residues are responsible for binding of the m^7G cap of mRNA. They also proposed that tryptophan-101 could participate in the binding. This proposal is consistent with the surface profile since Trp-101 very likely lies on the surface of the protein and therefore is a good candidate for a functional role in cap recognition. The pH profile for cap binding (Carberry *et al.*, 1991a) indicates that the binding site probably has an amino acid with a pK_a near 7.5; His-91 is a potential candidate for this residue even though it does not have such a high surface probability as Trp-101. From Chou-Fasman analysis, the region between residue 83-103 (containing His-91 and Trp-101) is a weak helical region and therefore could probably change conformation readily. Site-directed mutagenesis of the tryptophan residues in yeast 4E (Altmann *et al.*, 1988) revealed that two of the eight tryptophan residues (1 and 8) were required for cap binding activity. However, no determination of the structural consequences of these mutations was made so that it is unclear if these residues are actually involved in binding or are essential for proper folding of the protein.

Stopped-flow experiments were conducted using high concentrations of m^7GpppG and limiting concentrations of eIF-(iso)4F to ensure that the bimolecular combination of mRNA cap analogue with protein was pseudo first-order. The stopped-flow data

for the binding of m^7GpppG cap to the eIF-(iso)4F and p28 were plotted as ΔF *vs.* time as shown in Figure 4.8. Fitted curves correspond to the following single-exponential equation (Olsen *et al.*, 1993):

$$\Delta F = \Delta F_{\infty} [1-\exp(-k_{obs}t)]$$

where k_{obs} is the observed first-order rate constant, and the ΔF_{∞} is the maximum fluorescence change. The mechanisms considered involved a one- and a two-step binding process (Chapter 2).

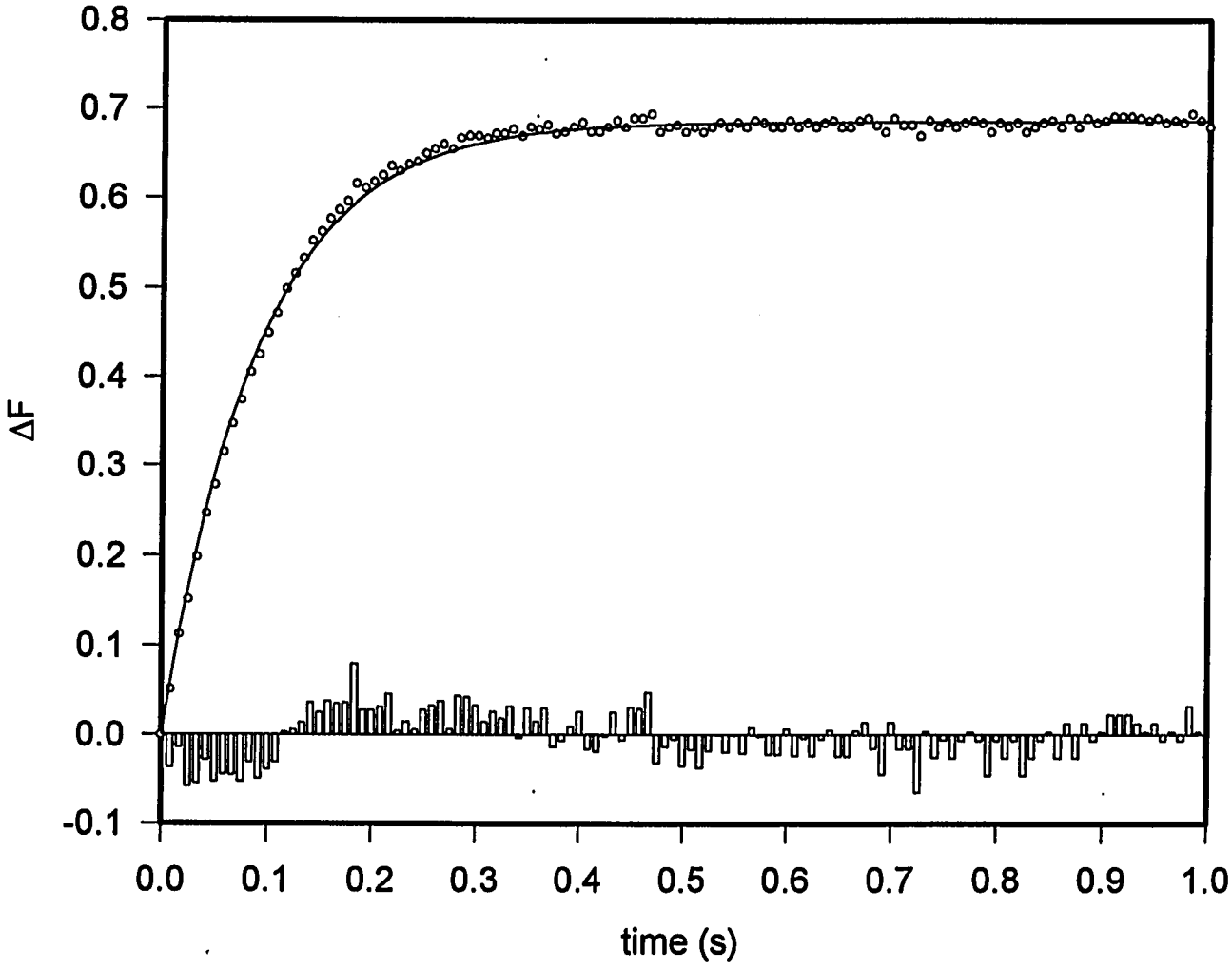

Figure 4.8. Single exponential curve fitting of the ΔF vs. time for the kinetics of 0.5 μM eIF-(iso)4F protein mixing with 5 μM m^7GpppG cap analog. k_{obs} is obtained form the fitted curve as 11.4 sec^{-1}. Bottom inset is the residuals of fitting amplified by 4 fold and plotted on the same x and y axis.

The interaction of eIF-(iso)4F (0.5 μM) with m^7GpppG under different concentrations of cap analog (2.5 μM, 5 μM and 10 μM) gave about the same k_{obs} (10.7 S^{-1}, 11.5 S^{-1}, and 12.1 S^{-1}, respectively). The reaction is not a single-step pseudo first order reaction (Chapter 2). The CD experiments have shown that eIF-(iso)4F undergoes conformational changes upon binding to m^7GpppG in agreement with Mechanism (ii),

$$P + C \underset{k_{-1}}{\overset{k_1}{\rightleftharpoons}} (P{\cdot}C)^* \underset{k_{-2}}{\overset{k_2}{\rightleftharpoons}} P{\cdot}C \qquad \text{(ii)}$$

so $$\frac{1}{k_{obs}} = \frac{1}{k_2} + \frac{K_1}{k_2[C]}$$

A plot of $\frac{1}{k_{obs}}$ vs $\frac{1}{[C]}$ will give an intercept of $1/k_2$ (Figure 4.9). This model gives a k_2 value of 12.2 sec^{-1}.

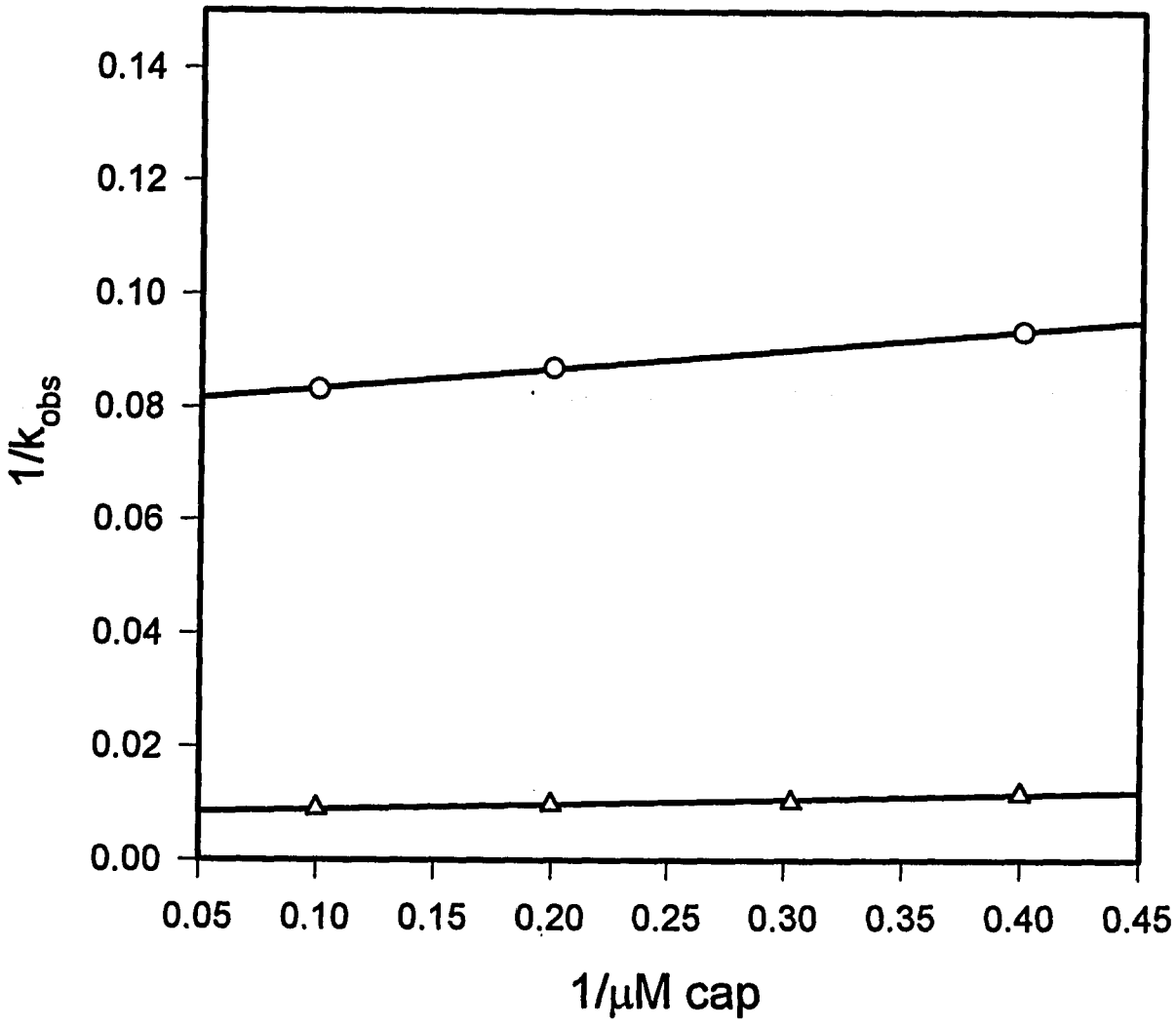

Figure 4.9. Kinetics plot of $1/k_{obs}$ vs 1/[C] of 0.5 μM eIF-(iso)4F (o) and p28 (Δ) under different m^7GpppG concentrations (2.5, 3.3, 5.0, 10.0 μM respectively).

k_2 was obtained as the reciprocal of Y intercept (12.2 sec^{-1} for eIF-(iso)4F and 123.3 sec^{-1} for p28).

Stopped-flow experiments of p28 binding with cap similar to those described above were also conducted. The CD experiments (data not shown) have shown that p28 undergoes conformational changes upon binding to m^7GpppG in agreement with Mechanism (ii). k_2 value of 123.5 sec^{-1} for p28 binding with the m^7GpppG cap analog was obtained. While more complex models with additional conformational changes will also fit the data, at present there are no experimental data to suggest such a mechanism is required. The two-step binding mechanism: a fast initial binding of relatively low affinity followed by a rather slow conformational change of the initial complex have been found in several cases (Silence *et al.*, 1992 & Sha, 1995). The second step rate constants were hundred folds differences. The studies of the interaction between the anti-cooperative bi-phasic binding of transcription factor USF to its cognate DNA (Sha *et al.*, 1995) gave about the same k_2 value as in the case of p28 with cap.

The stopped-flow kinetic data showed that the small subunit, p28, changed conformation approximately 10 times faster than eIF-(iso)4F (p28: k_2=123.5 s^{-1}, eIF-(iso)4F: k_2=12.2 s^{-1}). The faster conformational change rate of the p28-cap may be partially caused by an agile movement of its small mass (p28, 28 kDa compared to eIF-(iso)4F, 110 kDa). These results are surprising since one would expect p86 to increase the rate of complex formation, and hence increase the rate of interaction. However, if the initial equilibrium between the cap and protein is approximately the same for p28

and eIF-(iso)4F, then the off rate for eIF-(iso)4F would also be much slower than the off rate for p28. This would allow for interaction of other initiation factors or ribosome and favor formation of an active initiation complex.

One of the surprising aspects of this study is the ability of mRNA analogs to induce a large conformational change at pHs other than the optimal binding pHs. A literature search has not revealed other examples of such large changes in conformation where both conformations appear to be well ordered. It is interesting to speculate on the role of this large conformational change in activity of the protein. An analogy can be made to the hemoglobin-ligand conformational change where oxygen induces a large change in the protein conformational and affects the functional properties. In the hemoglobin case, however, the conformational change involves a "sliding" of the subunits and does not involve large changes in the α-helix and β-sheet content. Here, the active conformation of the protein appears to be the β-sheet conformation. It was reported earlier that protein phosphorylation is necessary for its effective function in translation and that phosphorylation is an important mechanism for regulation of protein synthesis in the cell (Minich *et al.*, 1994). Our study of protein phosphorylated and non-phosphorylated forms suggested that this conformational change seems to be affected by the post-translational modifications such as phosphorylation which affect activity. Recently Lin *et al.* (1994) showed that the mammalian cap binding protein, eIF-4E interacts with PHAS-1 in the signal transduction pathway of insulin. Protein-protein

interactions appear to play a significant regulatory role. Such large conformational changes as demonstrated here may be very important for affecting the protein-protein affinity and the corresponding affinity for cap and RNA leading to modulation of protein synthesis activity. Our results suggest a structural basis for changes in protein and cap affinity with pH and possibly other modifications.

Table 4.1 CD Spectral Analysis of eIF-(iso)4F & eIF-(iso)4F-Analog Complex at pH 6.3-8.6

pH 6.3	α-helix	β-sheet	β-turn	other
protein	42	14	21	23
protein+m^7GTP	34	23	26	17
protein+m^7GpppG	13	39	27	21
protein+oligo	13	45	30	12
protein +hairpin oligo	10	38	26	26
pH 7.0	**α-helix**	**β-sheet**	**β-turn**	**other**
protein	17	34	23	26
protein+m^7GTP	16	33	26	25
protein+m^7GpppG	11	44	26	19
pH 7.6	**α-helix**	**β-sheet**	**β-turn**	**other**
protein	15	38	22	25
protein+m^7GTP	13	57	22	8
protein+m^7GpppG	12	40	25	29
protein+oligo	9	38	24	26
protein+hairpin oligo	6	42	25	27
pH 8.0	**α-helix**	**β-sheet**	**β-turn**	**other**
protein	24	38	23	15
protein+m^7GTP	14	30	4	32
protein+m^7GpppG	11	50	22	17
pH 8.6	**α-helix**	**β-sheet**	**β-turn**	**other**
protein	35	29	26	10
protein+m^7GTP	30	21	25	24
protein+m^7GpppG	8	56	24	12

Table 4.2

Abundance of the secondary structure elements in p28 and p86 and their complex at pH 7.6

	α-helix	β-sheet	β-turn	other
	% amino acid residues			
p28	60	10	15	15
p28 + m^7GTP	21	31	23	25
p28 + m^7GpppG	8	37	26	29
p86	34	17	26	23
(p28+p86)/2[a]	47	13	20	20
p28/86[b]	30	20	24	26
p28/86(control)[c]	25	21	27	27
p28/86(pretreated)[d]	25	21	27	27
eIF-(iso)4F(dephosphorylated)[e]	24	28	26	23
eIF-(iso)4F	15	38	22	15

[a] The sum of p28 & p86. [b] Recombinant of p28 & p86. [c] Recombinant of p28 & p86 incubated with mRNA and ATP. [d] Recombinant of p28 & p86 incubated with eIF-4A, eIF-4B, eIF-3, mRNA and ATP. [e] Native eIF-(iso)4F treated with popato phosphatase acid.

Table 4.3

Estimation of the secondary structure for p28 by the method of Chou-Fasman (1978) (Table 4.3-a), and by the method of Ganier-Osguthorse-Robson (1978) (Table 4.3-b). The p28 amino acid sequence was taken from Allen *et al.* (1992).

a

α–helix		β-sheet	β-turn(or loop)	other
25-33 (9)[a]	47-53 (7)	7-11 (5)	12-22 (11)	
69-94 (26)	108-115 (8)	54-58 (5)	35-38 (4)	
140-150 (11)	153-159 (7)	99-104 (6)	42-46 (5)	
165-170 (6)	178-183 (6)	117-125 (9)	95-98 (4)	
189-194 (6)	220-233 (14)	208-218(11)	127-131 (5)	
236-245 (10)	252-257 (6)	246-251 (6)	173-177 (5)	
265-271 (7)	299-315 (17)	288-295 (8)	316-319 (4)	
320-328 (9)	344-364 (21)	329-342(14)	366-373 (8)	
374-381 (8)	389-394 (6)	382-387 (6)	415-421 (7)	
405-413 (9)	436-459 (24)	423-429 (7)	469-484 (16)	
516-524 (9)	560-568 (9)	536-540 (5)	487-494 (8)	
610-618 (9)	622-632 (11)	634-639 (6)	500-503 (4)	
640-651 (12)	655-662 (8)	663-667 (5)	512-515 (4)	
674-696 (23)	704-709 (6)	718-729(12)	525-534 (10)	
733-747 (15)	767-773 (7)	748-758(11)	555-559 (5)	
776-782 (7)			570-579 (10)	
			595-599 (5)	
(333)		(111)	(115)	(228)
42.3%		14.1%	14.6%	29.0%

b

α-helix	β-sheet	β-turn (or loop)	other
27-33 (7)	5-11 (7)	12-15 (4)	
79-94 (16)	23-26 (4)	35-38 (4)	
142-158 (17)	69-73 (5)	49-52 (4)	
205-213 (9)	188-193 (6)	61-68 (8)	
222-231 (10)	214-217 (4)	95-105 (11)	
239-257 (19)	404-410 (7)	127-137 (11)	
299-313 (15)	422-429 (8)	169-175 (7)	
319-332 (14)	466-469 (4)	178-182 (5)	
341-365 (25)	485-488 (4)	195-201 (7)	
372-383 (12)	536-541 (6)	258-273 (16)	
439-457 (19)	550-554 (5)	289-292 (4)	
608-648 (41)	558-568 (11)	366-369 (4)	
658-668 (11)	588-593 (6)	384-385 (4)	
675-698 (24)	603-607 (5)	395-403 (9)	
719-729 (11)	671-674 (4)	432-435 (4)	
734-755 (22)	699-711 (13)	470-473 (4)	
775-785 (11)		519-522 (4)	
		542-549 (8)	
(283)	(99)	(118)	
36.0%	12.6%	15.0%	36.5%

[a] The numbers in parentheses correspond to the total number of residues in the respective conformational forms.

Table 4.4

Comparison of predicted and measured secondary structure of p28 (Table 4.4-a) and p86 (Table 4.4-b)

a

Method	α-helix	β-sheet	β-turn (or loop)	other
	% amino acid residues			
CD, SELCON[a]	60.0	9.8	14.9	10.0
Chou-Fasman[b]	48.3	21.5	10.5	19.7
GOR[c]	36.8	13.9	23.4	25.9

b

Method	α-helix	β-sheet	β-turn (or loop)	other
	% amino acid residues			
CD, SELCON[a]	34.3	16.8	25.7	23.9
Chou-Fasman[b]	42.3	14.1	14.6	29.0
GOR[c]	36.0	12.6	15.0	36.5

[a] Spectral analysis through SELCON program (Sreerama & Woody, 1993) at pH 7.6. [b] Predicted by Chou-Fasman (1978) method. [c] Predicted by GOR method (Ganier & Osguthorse, 1978).

Chapter 5

Fluorescence and Circular Dichroism Spectroscopic Characterization of Wheat Germ Protein Synthesis Initiation Factor eIF-4F and its Subunit p26 with mRNA Cap Analogs

Except under unusual circumstances such as heat stress, nutrient deprivations or virus infection, it is believed that 48S complex formation, in which mRNA joins the 40S ribosomal subunit, is the rate-limiting step for protein synthesis (Rhoads, 1993 & Hershey, 1991). This process is catalyzed by group 4 initiation factors (Hershey, 1991 & Merrick, 1992) including eIF-4A, 4B and 4F. These polypeptides participate in binding the m^7G cap, unwinding mRNA secondary structure, and facilitating the movement of the 40S ribosomal subunit along the mRNA.

Mammalian eIF-4F is composed of three subunits of molecular masses 220, 45, and 26 kDa (Grifo *et al.*, 1983). eIF-4F isolated from wheat germ appears to differ both physically and functionally from mammalian eIF-4F. Wheat germ eIF-4F is a high molecular weight complex that contains two major polypeptides (220 and 26 kDa) in a 1:1 molar ratio and no detectable 46-50-kDa polypeptide (Lax *et al.*, 1985 & 1987). p26, the small subunit of eIF-4F, occasionally referred to as eIF-4E, has been cloned from human (Rychlik *et al.*, 1987), yeast (Altman *et al.*, 1988), and mouse (Altman *et al.*, 1987) cells with extensive sequencing of peptides from the rabbit protein (Rychlik *et al.*, 1987). Several studies led to the suggestion that the initial binding of eIF-4F to the mRNA occurs via p26 subunit recognition of the m^7G cap structure at the 5' end of eukaryotic mRNAs (Edery *et al.*, 1987; Grifo *et al.*, 1984; Rhoads *et al.*, 1985; Sonenberg *et al.*, 1979; Tahara *et al.*, 1981; & Webb *et al.*, 1984).

Recently the purified subunit p26, a cap binding protein, has been obtained from *E. coli.* expression of the cloned DNA. Here, we present a study of the biophysical properties of eIF-4F and p26 by employing fluorescence and circular dichroism spectroscopy on a protein-cap complex system, aimed at enhancing our understanding of the structure-function relationship of these initiation factors.

5.1 Experimental Procedure

5.1.1. Fluorescence Titration

The fluorescence equilibrium binding studies were carried out on a SPEX Fluorolog-2 Spectrofluorometer in buffer A: 20 mM HEPES-KOH, 1 mM DTT and 1 mM $MgCl_2$ at the pH indicated. All chemicals were reagent grade or better.

The intrinsic fluorescence of p26 and eIF-4F were used to monitor binding of cap analos. An excitation wavelength of 290 nm, the excitation and emission slits 1.4 mm and a 1 cm pathlength were employed. All fluorescence measurements were carried out at 23°C unless otherwise noted. Other details of the titration experiments and data analysis are described elsewhere (Carberry *et al.*, 1989 and 1990).

5.1.2. Solute Accessibility Studies

The quenching of p26 and eIF-4F with different quenchers was followed by titration with aliquots of 5.0 M potassium iodide, 6.7 M trichloroethanol and 2.5 M thallium acetate. Fluorescence dynamic quenching occurs during the excited-state lifetime of the fluorophore as a result of the random collisions of quenching ligand (Q) and the fluorophore (Parker, 1968 & Lakowicz, 1983). In the absence of a static component,

the deactivation of the excited state of the fluorophore is described by the following equation:

$$Fo/F = 1 + K_{sv}[Q]$$

where *Fo* and *F* are the fluorescence intensities in the absence and presence of the quenching ligand at concentration [Q]. K_{sv} is the Stern-Volmer quenching constant, the product of the bimolecular quenching rate constant and the fluorescence lifetime of the fluorophore.

5.1.3. Circular Dichroism

The CD experiments were performed on Jasco-710 spectropolarimeter using circular cells with a 0.5 mm pathlength. Samples were prepared at a concentration of about 0.2 mg/mL in Buffer B, 20 mM HEPES-KOH, 0.1 mM EDTA, 10% glycerol and 100 mM KCl at room temperature. All the experimental conditions were the same as described elsewhere (Wang *et al., in preparation*). Estimation of the secondary structure for the CD data, expressed as mean residual ellipticity, was made with the program SELCON (Sreerama & Woody, 1993).

5.1.4. Stopped-flow Kinetics

The kinetics of the interaction between eIF-4F and cap analog were monitored the intrinsic protein fluorescence changes after rapid mixing by a Hi-Tech Scientific SFA-11 stopped-flow apparatus. The excitation and emission wavelengths were 290 and 335 nm, respectively with 1 ms integration time. The slitwidth was 2 mm. After rapid mixing m^7GpppG cap with eIF-4F, the fluorescence time course was recorded. The plots were fitted by the nonlinear analytical equations in the Sigmaplot program from Jandel Scientific.

5.2 Results

5.2.1 Fluorescence of p26•cap Complex

The fluorescence emission spectra of p26•cap complexes are shown in Figure 5.1. The spectra were characterized by a maximum near 332 nm. Addition of cap analog produced a dramatic decrease in protein fluorescence intensity at all wavelengths. This reduction in intensity is probably a consequence of stacking interactions of tryptophan and the nucleic acid base (Ishida *et al.*, 1983; Brun *et al.*, 1975; Lawaczek & Wagner, 1974). Since the position of emission maximum of the spectra (332 nm) was close to that of free tryptophan residue (348 nm), it indicated that tryptophans are involved in the binding. The relative fluorescence intensity changes at 332 nm in free and complex p26 emission spectra were utilized to calculate the binding constants Keq for p26•m^7GTP according to the Eadie-Hofstee equation, shown in the inset of Figure 5.1.

5.2.2. pH Dependence

The binding of cap to protein was sensitive to pH. The bell-shaped pH-dependent binding profile for p26•m^7GTP reported here (Figure 5.2) had the same shape as that

of eIF-4F•m^{7}GTP (Carberry *et al.*, 1991a & b). Both of them showed the optimum binding condition at pH 8.0, compared with the pH optimum of 7.05 (Sha *et al.*, 1995) for p28•m^{7}GTP complex and 7.6 for eIF-(iso)4F•m^{7}GTP complex (Carberry *et al.*, 1991a & b). This binding feature probably reflected titration of an amino acid residue with a pKa near pH 8.0.

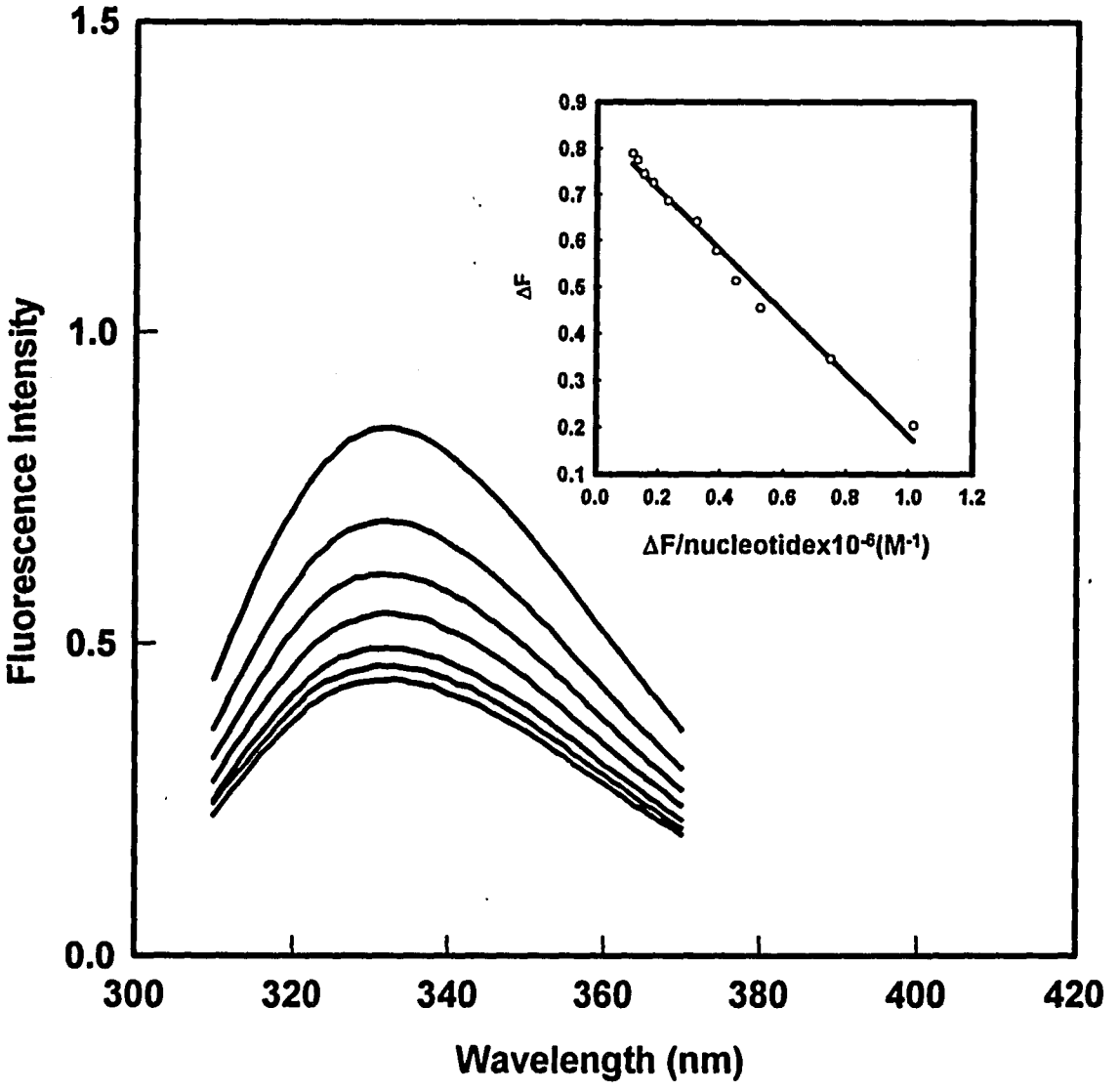

Figure 5.1. Fluorescence emission spectra of p26 subunit of wheat germ eIF-4F (0.5μM) titrated with cap analog m^7GTP in buffer A, pH 8.0 at 23 °C. The cap concentration (from top to bottom) was 0, 0.1,0.2, 0.5,1.0,1.2,2.0 μM. The excitation wavelength was 290 nm, and 1.4 mm slit was employed. Emission maxima was observed at 332 nm. Inset: Eadie-Hofstee plot of fluorescence data. ΔF was calculated at 332 nm where $\Delta F=F_{p26}-F_{p26+cap}$.

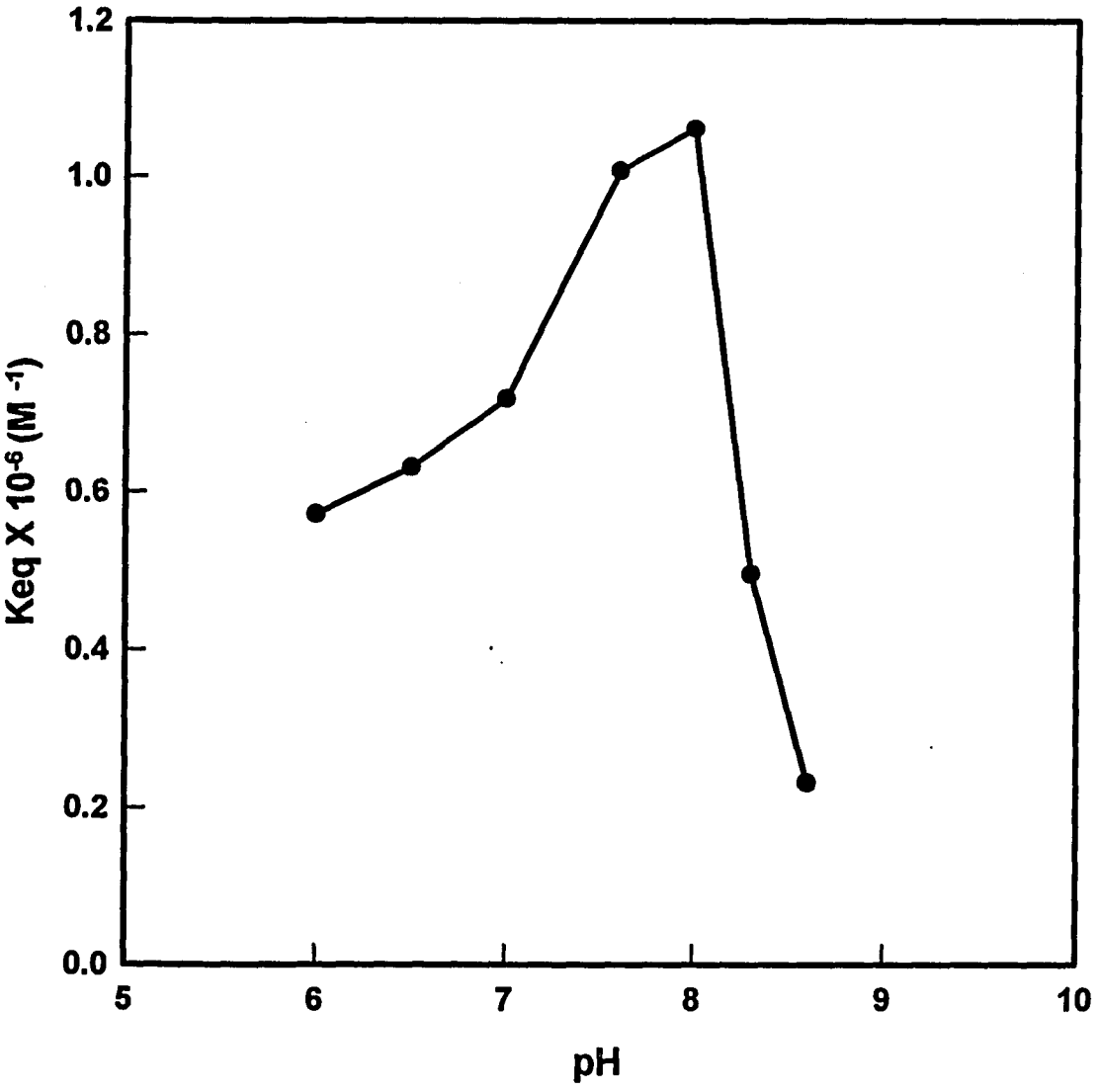

Figure 5.2. Binding of m^7GTP and p26 as a function of pH. All solutions were prepared in buffer A, adjusted to the appropriate pH at 23°C. Other conditions were the same as in Figure 5.1.

5.2.3. Temperature Dependence

Utilizing K_{eq} values obtained from fluorescence measurement at different temperatures, van't Hoff plots give ΔH=10.23 kcal/mol, ΔS=57.33 cal/mol°C (shown in Figure 5.3). These values are larger than those of p28•m^7GTP (Sha *et al.*, 1995) and eIF-4F•m^7GTP (Carberry *et al.*, 1991a). The positive values of ΔH and ΔS may be accounted for by either hydrophobic (Gill *et al.*, 1967 & 1976) or ionic (Pimentel & McClellan, 1971) interactions. Different quenchers were applied to this system in order to investigate the binding site environment.

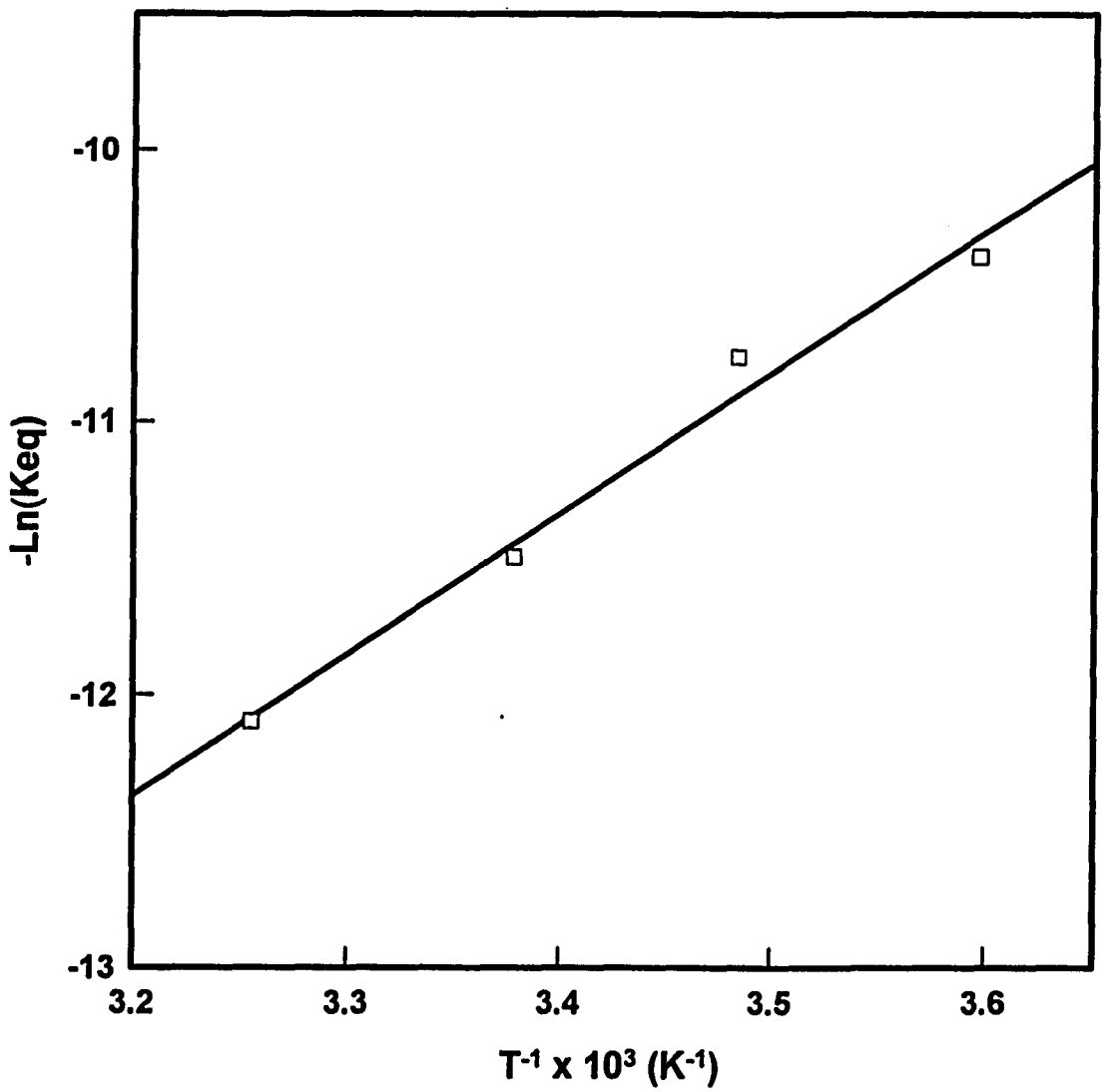

Figure 5.3. van't Hoff plot for p26-m^{7}GTP interactions. All experimental conditions were in Figure 5.1.

5.2.4. Solvent Accessibility and Environment of the Tryptophan Residues in p26 & eIF-4F

The Stern-Volmer plot for fluorescence quenching of p26 and eIF-4F in solution by CCl_3CH_2OH (TCE) is shown in Figure 5.4. The linear character of the plot suggested that only a single class of tryptophan residue is quenched. This is further supported by a lack of wavelength shift and constant shape of the emission in the presence of the quencher (spectra not shown). More information about the nature of the location of the tryptophan residues in p26 and eIF-4F can be obtained by studying the quenching by ionic quenchers. Two quenchers particularly useful in studying tryptophan fluorescence are the negatively charged iodide (I^-) and the positively charged thallium (Tl^+) ions. The Stern-Volmer quenching constants (Stern & Volmer, 1919) by trichloroethanol, Tl^+ and I^- are included in Table 5.1. It is noticed that there are striking differences between these selected quenchers. The larger values of quenching constants of TCE for both proteins strongly suggest that tryptophan residues of p26 and eIF-4F are located in a hydrophobic environment and that the high quenching efficiency of TCE results from preferential "recognition" of hydrophobic domains by the quenchers. While Tl^+ is, by a factor of ~7.3, less efficient when compared with trichloroethanol, Tl^+ is ~8.3 times more efficient in quenching p26 fluorescence than I^-;

this suggests that there are negatively charged groups of amino acids in close proximity to tryptophan residues in p26 and eIF-4F (Lakowicz, 1983).

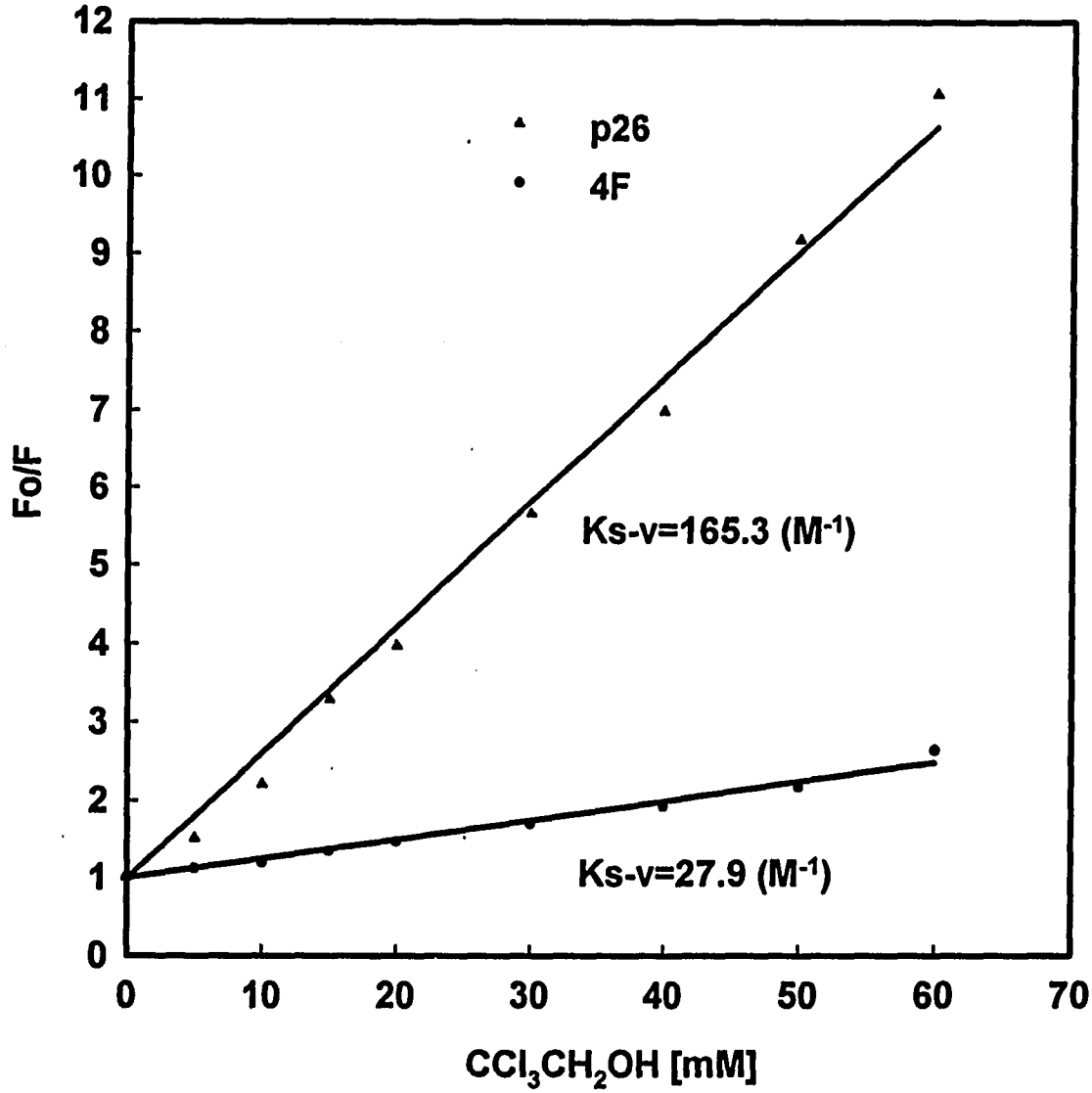

Figure 5.4. Stern-Volmer plot of CCl_3CH_2OH quenching to p26 and eIF-4F

All experimental conditions were the same as in Figure 5.1.

5.2.5 Stopped-flow Fluorescence Kinetics

Since the fluorescence of eIF-4F decreases with time upon its rapid mixing with m^7GpppG, the elementary steps involved in these interactions were evaluated by stopped-flow spectrofluorimetry.

The observed rate constants k_{obs} were measured by performing the experiment using at least 10-fold higher concentration of cap than the concentration of the eIF-4F to maintain the pseudo-first order kinetic conditions. A representative stopped-flow fluorescence trace of time-dependent change in fluorescence of eIF-4F upon its rapid mixing with cap is shown in Figure 5.5. The observed rate constant, k_{obs}, was evaluated from the slopes of linear plots of ln (ΔF_t - ΔF_∞) versus time (t) where ΔF_t and ΔF_∞ are fluorescence changes at time t and time infinite, respectively. The first mechanism listed in Chapter 2 (Equation 1.2.1)

$$P + C \underset{k_{-1}}{\overset{k_1}{\rightleftharpoons}} P{\cdot}C \qquad \text{(i)}$$

$$k_{obs} = k_{-1} + k_1[C] \qquad (1.2.1)$$

was ruled out by fitting k_{obs} versus [C]. The representative plot of k_{obs} versus [C] used for determination of k_2 for eIF-4F from the intercept at 9.5°C is shown in Figure 5.6. The activation energy for the second step 4.55 $kcalmol^{-1}$ was obtained from the Arrhenius plot (shown in Figure 5.7).

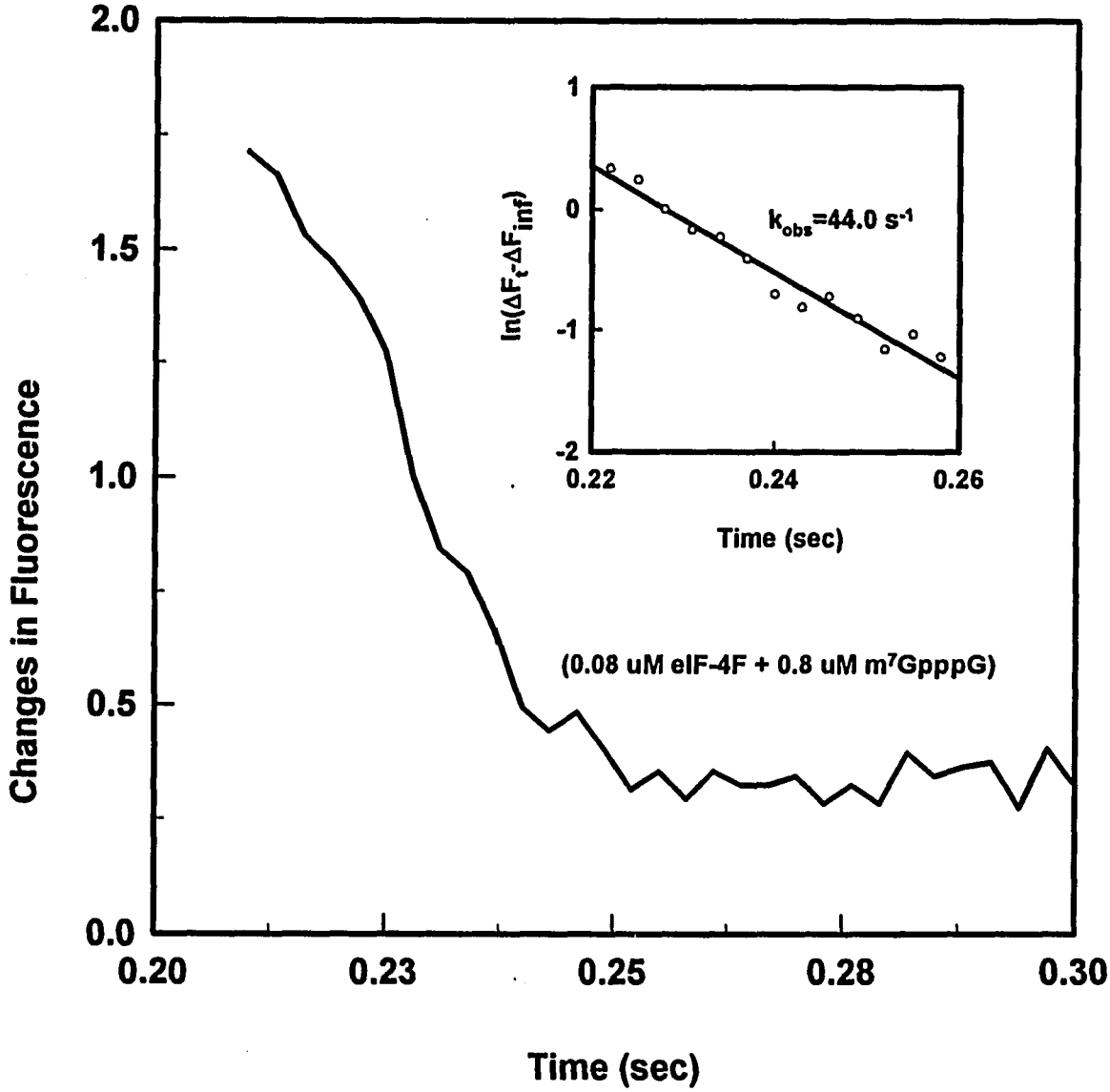

Figure 5.5. A stopped-flow fluorescence trace of eIF-4F upon rapid mixing with m^7GpppG at 9.5°C. eIF-4F (0.08μM) and m^7GpppG (0.8μM) were allowed to mix in equal amounts in a stopped-flow instrument. The sample were excited at 290 nm, and emission were recorded at 332 nm. The inset represents a plot drawn according to the regression equation, the slope of that yields k_{obs} of 44.0 s^{-1}.

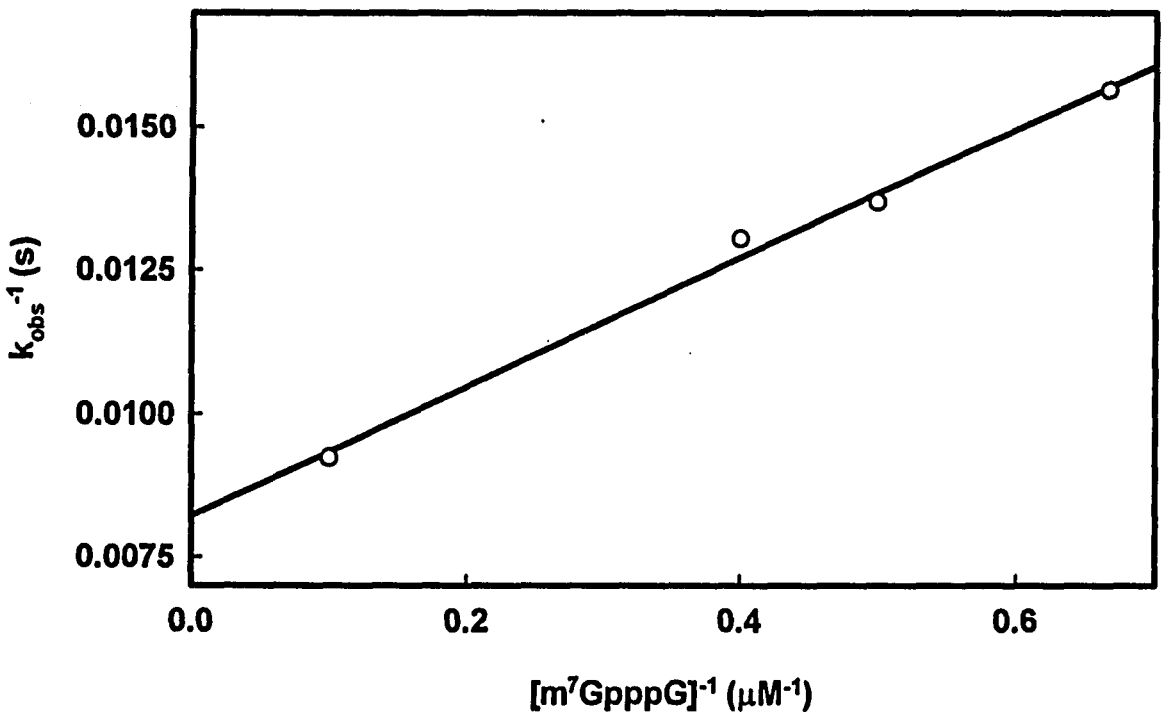

Figure 5.6. Kinetic plot of $1/k_{obs}$ vs. 1/[m^{7}GpppG]. The concentration of eIF-4F was 0.4 μM. k_2 was obtained from the reciprocal of Y intercept (121.7 s^{-1}).

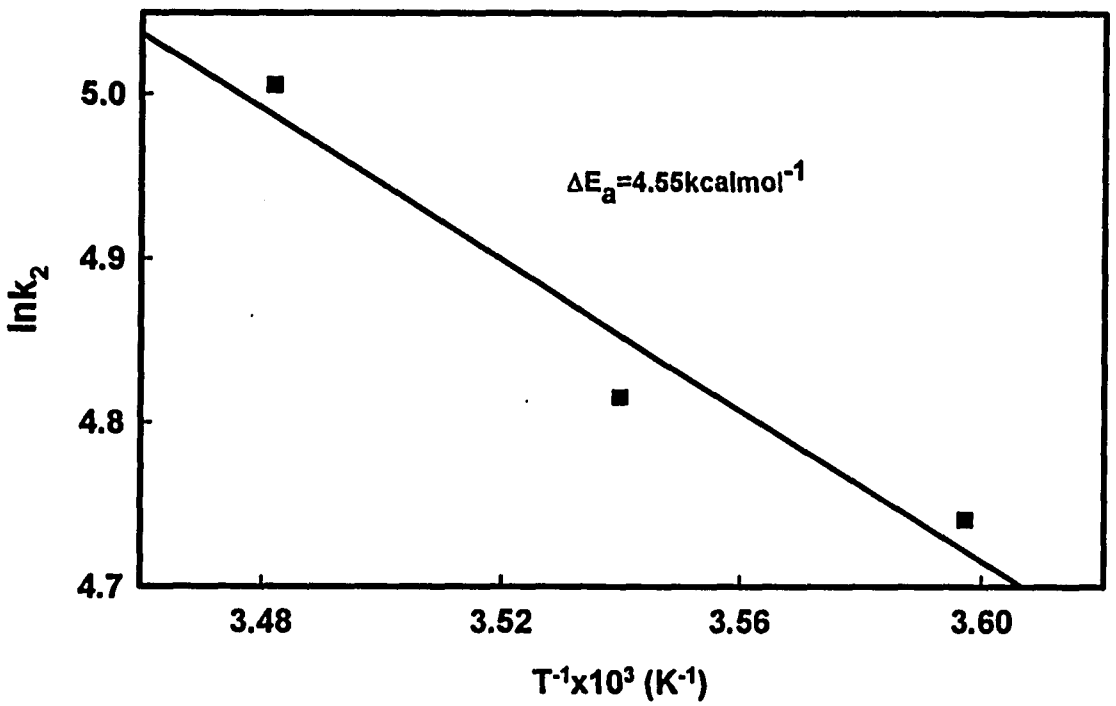

Figure 5.7. Arrhenius Plot of k_2 for eIF-4F-m^{7}GpppG. The experiment was carried out at 5°C, 9.5°C and 15°C.

5.2.6 CD Studies of p26 and eIF-4F

The CD spectra of eIF-4F and p26 are shown in Figure 5.8 and Figure 5.9, respectively. It is noticed that eIF-4F and p26 lack any significant changes under different pH conditions. The spectrum of eIF-4F is characterized by minima at 208 and 222 nm, which indicates the rich α-helical content, while p26 seems to have more β-sheet structure, similar to the spectrum of yeast eIF-4E (McCubbin *et al.*, 1988). The estimation of the secondary structural elements within eIF-4F and p26 by applying SELCON program (Sreerama & Woody, 1993) are included in Table 5.2. The ~38% of α-helix and ~17% of β-sheet within eIF-4F compared with ~15% of α-helix and ~36% of β-sheet within p26 can be expected. It can be seen that the CD spectra (Fig.5.8 & 5.9) remain almost the same in the presence of cap analogues. It appears that the protein conformational changes caused by cap analogs very probably occur only at the tertiary structural level but not at the secondary structural level.

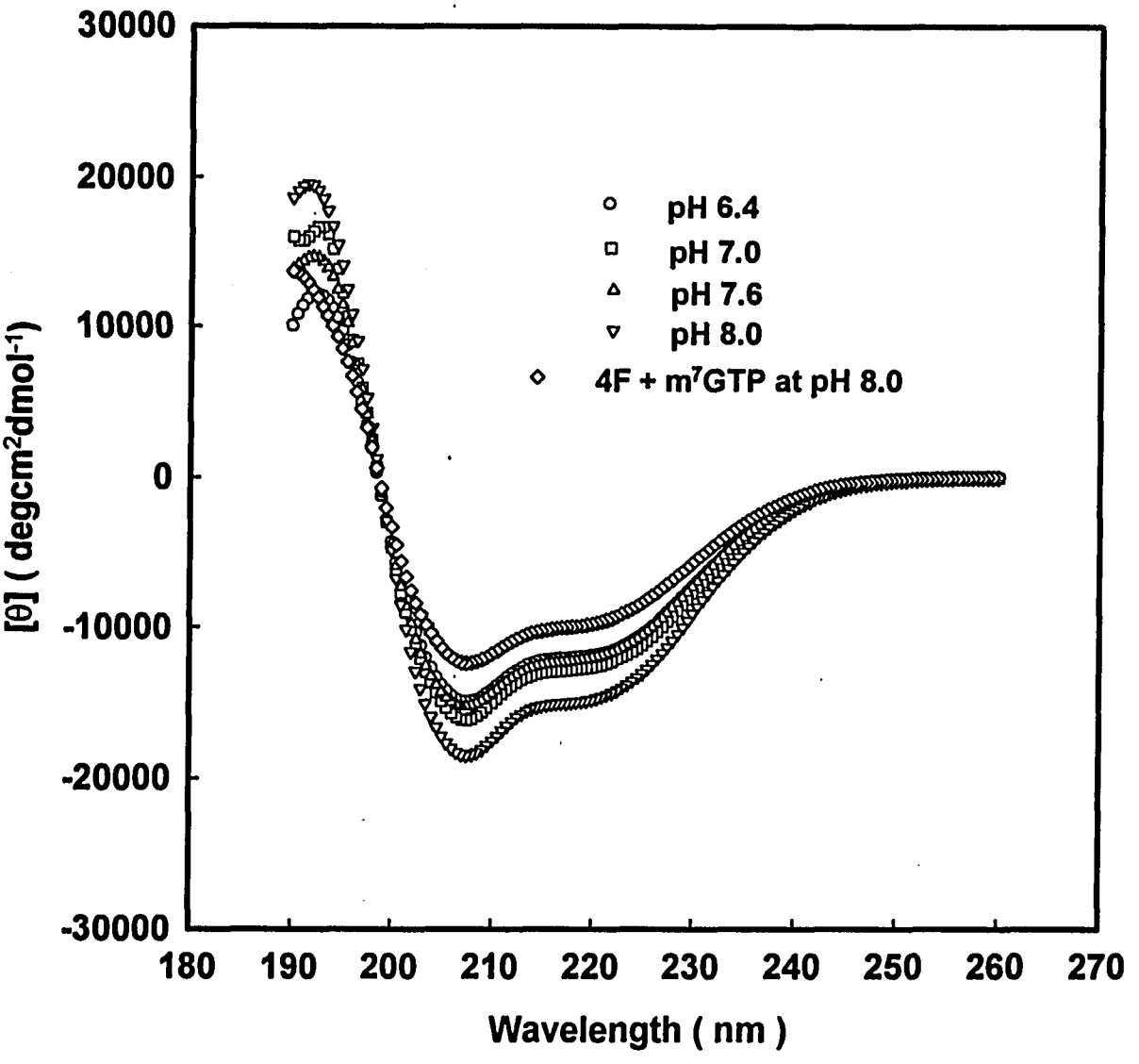

Figure 5.8. CD spectra of eIF-4F. The solvent system was 20 mM HEPES-KOH, 0.1 mM EDTA, 1 mM DTT, 10% glycerol, and 120 mM KCl. The concentration of eIF-4F was 0.2 mg/mL.

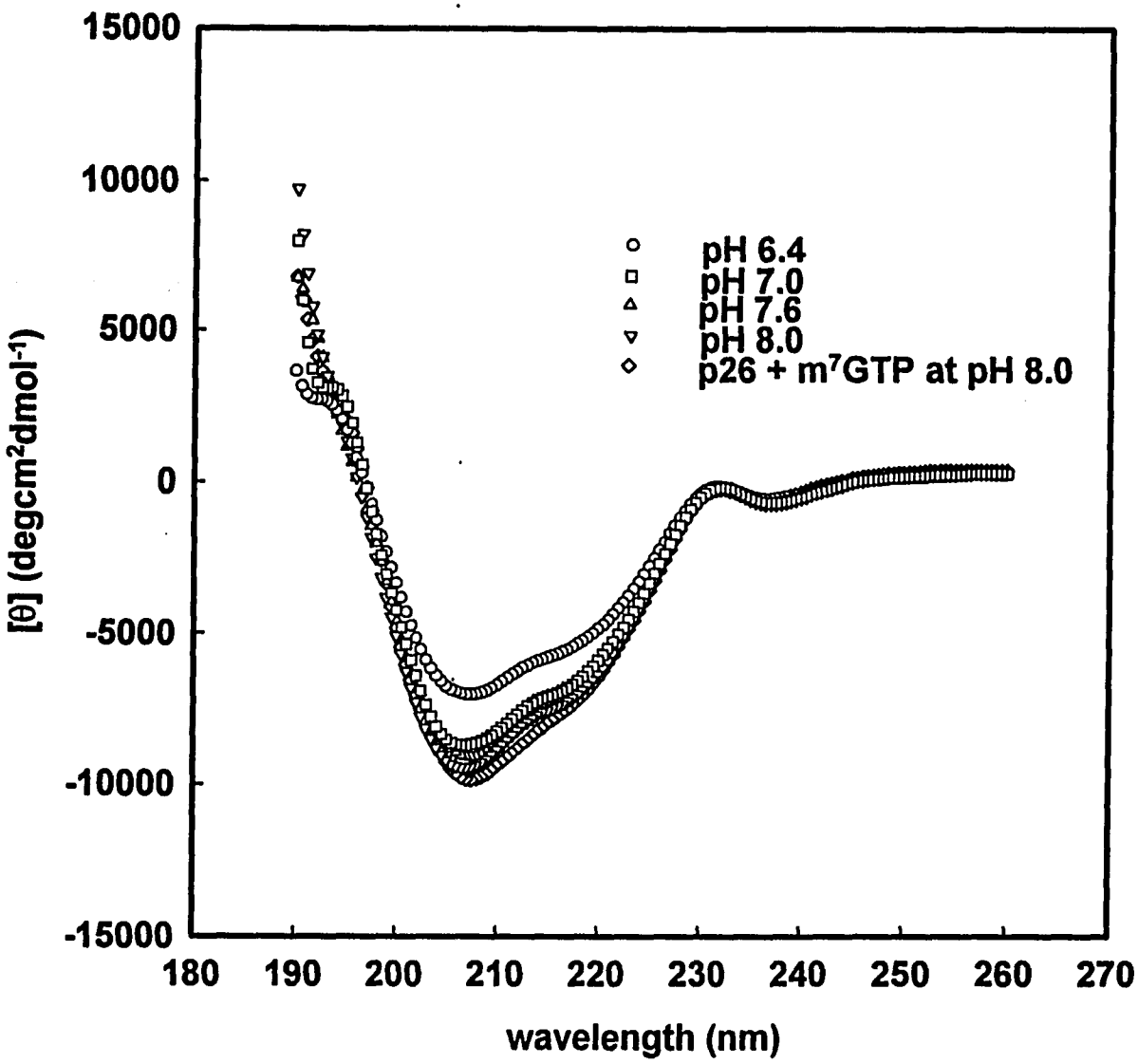

Figure 5.9. CD spetra of p26. The concentration of p26 was 0.2 mg/mL. The experimental conditions were the same as in Figure 5.8.

5.3 Discussion

The ability of a protein to recognize a specific sequence of bases along a strand of DNA or RNA is a fundamental biological process. Aromatic amino acids can bind with nucleic acids via π-π stacking interaction. Among them, tryptophan has the strongest binding ability because of the best π-electron donation character of the indole ring at its side chain. In this study, the interactions of p26 and eIF-4F with m^7G were carried out by monitoring either the fluorescence static or kinetic changes of tryptophan residues upon cap binding.

The fluorescence emission maximum of complex p26•m^7GTP occurs near 332 nm, a figure indicative of somewhat buried tryptophan fluorophores. The effect revealed that tryptophan residues were probably involved in the binding with cap analog since the emission maximum 332 nm in the complex was close to the tryptophan free form 348 nm. This phenomenon was observed in the studies for human 4E (Carberry, *et al.*, 1989), wheat germ eIF-4F, eIF-(iso)4F (Carberry *et al.*, 1991a & b) and its subunit p28 (Sha *et al.*, 1995) as well.

The pH dependent binding profile of p26 is bell-shaped, similar to eIF-4E (Carberry *et al.*, 1989) and p28 of eIF-(iso)4F (Sha *et al.*, 1995). Carberry *et al.* (1989) proposed

that the increase in K_{eq} at pH values below the optimum was due to the increased affinity of a protonated histidine residue with the enolate form cap while the decreased K_{eq} values at pH greater than optimum was due to the decrease in the affinity of the deprotonated histidine residue with the cap. Two pK_as accounted for these interactions: one for cap (pKa=6.04) and one for histidine (pKa=6-8).

The localized conformational changes were also monitored by probing the accessibility of tryptophan residues to collisional quenchers such as potassium iodide, thallium acetate and trichloroethanol. The information about the nature of the location of the tryptophan residues in p26 and eIF-4F can be examined by different quenchers. Since trichloroethanol is a known hydrophobic quencher of protein fluorescence (Eftink *et al.*, 1977 & Eftink, 1991), it can be expected that the quencher will sense the presence of a hydrophobic domain in the vicinity of tryptophan residues. The negatively charged iodide (I^-) and the positively charged thallium (Tl^+) ion were selected as the ionic quenchers. Both quenchers have similar diffusion coefficients and their indole fluorescence quenching efficiencies equal ~1 (Ando & Asai, 1980; Eftink, 1991). The linear character of the Stern-Volmer plots (Fig. 5.4) and the lack of any significant changes in the protein emission spectra (spectra not shown) in the presence of the quenchers with dramatically different physical properties suggest that tryptophan residues of eIF-4F form a single class of residues located in a similar environment. There are significant differences between the Stern-Volmer plots of these two

quenchers. The larger quenching effect by Tl^+ indicates that the tryptophan residues in p26 and eIF-4F are located in a predominantly negatively charged hydrophobic region, which suggests the charge repulsion between PO_4^{3-} of cap and the binding site are not important. Our results are consistent with earlier proposal that the cap binding protein should contain a Trp residue and the binding site tryptophan might be located around the negatively charged amino acid at the binding sites for the capped mRNA (Ishida *et al.*, 1983 and Ueda *et al.*,1991a & b). Inspecting the sequence of p26 (Figure 5.10) with these considerations in mind, Trp-5 would be a suitable candidate.

It is obvious that the interactions between p26, eIF-4F and m^7G cap are accompanied only by subtle changes in the protein conformation from the CD spectra. The fitting of the stopped-flow fluorescence trace demonstrated that the kinetics follow a two-step mechanism, in which a protein conformational change is involved upon complex formation. Unlike the interaction of eIF-(iso)4F and its subunit p28 with mRNA analogs (Wang *et al, in preparation*), such conformational changes in the systems p26, eIF-4F with m^7G cap analog do not occur at the secondary structural level (Fig. 5.8, Fig. 5.9 & Table 5.2). The same observations can be found in an earlier study of yeast eIF-4E (McCubbin *et al.*, 1988) where no dramatic secondary structure changes in eIF-4E were shown in the presence of cap analogs, and studies of the binding of dyes to cyclodextrins and ligands to Jacalin (Gupta *et al.*, 1992), where the role of steric factors have been demonstrated. A similar case was also described in the hemoglobin-

oxygen system in which the conformational change in hemoglobin does not exhibit the changes of the α helical or β sheet contents but involves a "sliding" of the subunits. The relatively large enthalpy value involved in the binding of p26 to m^7G cap analogue could be utilized to overcome these steric constraints, such as conformational changes in protein and protein-cap complex.

p26 (wheat germ):

1 ---------- ----- - EGEIA DDGDGSSAAA AGRITA**H**PLE
His

43 NA**W**TF**W**FDNP -QGKSR- QVA**W**G STI**H**PI**H**TFS TVEDF**W**GLYN
Trp 1 Trp2 Trp3 His His Trp4

83 NI**H**NPSKLNV GADF**H**CFKNK IEPKWEDPIC ANGGKW- - T
His His Trp 5 Trp6

123 ISCGR - GKSD TF**W**L**H**TLLAM IGE-QF-DFG DEICGAVVSV
Trp7 His

163 RQKQERVAI**W** TKNAAN- EAA QISIGKQ**W**KE FLDYKDS- - I
Trp 8 Trp 9

203 GFIV**H**EDAK- RSDKGPKNRY TV
His

Figure 5.10 Amino acid sequence of p26 subunit of wheat germ eIF-4F. Histidine and tryptophan residues are in bold and labeled. Numbers are started from N-terminal. Metz *et al.*, 1992.

Table 5.1

Quenching constants of p26 and eIF-4F fluorescence by different ligands

Quenching constant	Quencher					
	Cl_3CCH_2OH		I^-		Tl^+	
	p26	4F	p26	4F	p26	4F
K_{sv} $(M^{-1})^a$	165.3	27.9	2.7	2.6	22.5	10.2

[a] Excitation and emission wavelengths were at 290 and 332 nm, respectively.

Table 5.2

CD spectral analysis of eIF-4F & p26

	α-helix	β-sheet	β-turn	other
eIF-4F	38	17	26	19
eIF-4F + m^7GTP	31	18	27	24
p26	15	36	28	21
p26 + m^7GTP	17	35	28	20

References

Abramson, R. D., Browning, K. S., Dever, T. E., Lawson, T. G., Thach, R. E., Ravel, J. M., and Merrick, W. C. (1988) *J. Biol. Chem.* ***263***, 5462-5467.

Allen, M. L., Metz, A. M., Timmer, R. T., Rhoads, R. E., and Browning, K. S. (1992) *J. Biol. Chem.* ***267***, 23232-23236.

Altmann, M., Edery, I., Trachsel, H., and Sonenberg, N. (1988) *J. Biol. Chem.* ***263***, 17229-17232.

Altmann, M., Handschin, C., and Trachsel, H. (1987) *Mol. Cell. Biol.* ***7***, 998-1003.

Ando, T., and Asai, H. (1980) *J. Biochem. (Tokyo)* ***88***, 255-264.

Brahms, S., and Brahms, J. (1980) *J. Mol. Biol.* ***138***, 149-178.

Browning, K.S., Lax, S. R., and Ravel, J. M. (1987) *J. Biol. Chem.* ***262***, 11282-11292.

Browning, K.S., Webster, C., Roberts, J. K. M., and Ravel, J. M. (1992) *J. Biol. Chem.* ***267***, 10096-10100.

Brun, F., Toulme, J.-J., and Helene, C. (1975) *Biochemistry 14*, 558-563.

Bujalowski, W. and Lohman, T. M. (1986) *Biochemistry 25*, 7799-7802.

Bujalowski, W. and Lohman, T. M. (1987) *Biochemistry 26*, 3099-3106.

Burd, C. G., and Dreyfuss, G. (1994) *Science 265*, 615-621.

Carberrry, S. E., Darzynkiewicz, E., and Goss, D. J. (1991a) *Biochemistry 30*, 1624-1627.

Carberry, S. E., Darzynkiewicz. E., Stepinski, J., Tahara, S. M., Rhoads, R. E., and Goss, D. J. (1990) *Biochemistry 29*, 3337-3341.

Carberry, S. E., Friedland, D. E., Rhoads, R. E., and Goss, D. J. (1992) *Biochemistry 31*, 1427-1432.

Carberry, S. E., and Goss, D. J. (1991b) *Biochemistry 30* , 4542-4545.

Carberry, S. E., Rhoads, R. E., and Goss D. J. (1989) *Biochemistry 28*, 8078-8083.

Chou, P. Y., and Fasman, G. D. (1978) *Adv. in Enzymol. 47*, 45-148.

Edery, I., Pelletier, J., and Sonenberg N. (1987) *Translational Regulation of Gene Expression* 335-366.

Edery, I., and Sonenberg, N. (1985) *Proc. Natl. Acad. Sci. USA 82*, 7590-7594.

Eftink, M. R.(1991) in *Biophysical and Biochemical Aspects of Fluorescence Spectroscopy* (Deway, T. G., ed) pp.1-41, Plenum Press, New York.

Eftink, M. R., Zajicek, J. L., and Ghiron ,C. A. (1977) *Biochi. Biophys. Acta 491*, 473-481.

Emini, E. A., Hughes, J. V., Perlow, D. S., and Boger, J. A. (1985) *J. Virol. 55*(3), 836-839.

Fersht, A. 1984, *Enzyme Structure and Mechanism*, 2nd Ed. pp 121-143, W. H. Freeman and Company.

Furuichi, Y., LaFiandra A., and Shatkin, A. J. (1977) *Nature (London) 266*, 235-239.

Ganier, J., and Osguthorse, D. J. (1978) *J. Mol. Biol. **120***, 97-120.

Gill, S. J., Downing, M., and Sheats, G. F. (1967) *Biochemistry 6*, 272-276.

Gill, S. J., Nichols, N. F., and Wadso, I. (1976) *J. Chem. Thermodyn. **8***, 445-452.

Gorlach, M., Wittekind, M., Beckman, R. A., Mueller, L., and Dreyfuss, G. (1992) *EMBO J. **11***, 3289-3295.

Goto, Y., and Amito, S. (1991) *J. Mol. Biol. **218***, 387-396.

Grifo, J. A., Abramson, R. D., Satler, C. A., and Merrick, W. C. (1984) *J. Biol. Chem. **259***, 8648-8654.

Grifo, J. A., Tahara, J. P., Leis, M. A., Morgan, A. J., Shatkin, A. J., and Merrick, W. C. (1983) *J. Biol. Chem. **258***, 5804-5810.

Gupta, D., Rao, N. V, S. A. V. P., Puri ,K. D., Matta, K. L., and Surolia, A. (1992) *J. Biol. Chem. **267*** (13) 8909-8918.

Hart, R. P., McDevitt, M. A., and Nevins, J. R. (1985) *Cell 43*, 677-683.

Henshaw, E. C., Hirsch, C. A., Morton, B. E., and Hiatt, H. H. (1971) *J. Biol. Chem. 246*, 436-446.

Hershey, J. W. B (1991) *Annu. Rev. Biochem. 60*, 717-755.

Hopp, T. P., and Woods, K. R. (1981) *Proc. Natl. Acad. Sci. U. S. A. 78*, 3824-3828.

Ishida, T., Katsuta, M., Inoue, M., Yamagata, Y., & Tomita, K. (1983) *Biochem. Biophys. Res. Commun. 115*, 849-854.

Jagus, R., Anderson, W. F., and Safer, B. (1981) *Prog. Nucleic Acid Res. Mol. Biol. 25*, 127-185.

Konarska, M. M., Padgett, R. A., and Sharp, P. A. (1984) *Cell 38*, 731-736.

Lakowicz, J. R. (1983) *Principle of Fluorescence Spectroscopy*, pp 319-484, Plenum Press, New York.

Lawaczek, R., and Wagner, K. G. (1974) *Biopolymers 13*, 2003-2014.

Lax, S., Fritz, W., Browning, K. S., and Ravel, J. (1985) *Proc. Natl. Acad. Sci. U.S.A.* ***82***, 330-333.

Lax, S. R., Browning, K. S., Maria, D. M., and Ravel, J. M. (1987) *J. Biol. Chem.* ***261***, 15632-15636.

Lin, T. -A., Kong, X, Haystead, T. A. J., Pause, A., Belsham, G., Sonenberg, N., and Lawrence., J. C., Jr. (1994) *Science* ***266***, 653-656.

Manavalan, P., and Johnson, W. C., Jr. (1983) *Nature (London)* ***305***, 831-832.

McCarthy, J. E. G., and Kollmus, H. (1995) *TIBS* ***20***, 169-215.

McCubbin, W. D., Edery, M., Altmann, M., Sonenberg, N., and Kay, C. M. (1988) *J. Biol. Chem.* ***263***, 17663-17671.

McCubbin, W. D., Edery I., Altmann, M., Sonenberg, N., and Kay, C. M. (1989) *FEBS Lett.*, ***245***, 261-266.

Merrick, W. C. (1992) *Microbiol. Rev.* ***56***, 291-315.

Merrick, W. C. (1994) *Biochimie 76*, 822-830.

Metz, A. M., Timmer, R. T., and Browning, K. S. (1992) *Nucleic Acid Res. 20*, 4096.

Minich, W. B., Balasta, M. L., Goss, D. J., and Rhoads, R. E. (1994) *Proc. Natl. Acad. Sci. USA, 91*, 7668-7672.

Olsen, K., Christensen U, Sierks, M. R., and Svensson, B. (1993) *Biochemistry 32*, 9686-9693.

Parker, C. A. (1968) *Photoluminescence of Solutions*, Elsevier Science Publishers B. V., Amsterdam.

Pause, A. and Sonenberg, N. (1992) *EMBO J., 11*, 2643-2654.

Pimentel, G. C., and McClellan, A. L. (1971) *Annu. Rev. Phys. Chem. 22*, 347-358.

Ray, B., Lawson, T., Kramer, J., Cladaras, M., Grifo J., Abramson, R. D., Merrick, W. C., and Thach, R. E. (1985) *J. Biol. Chem. 260*, 7651-7658.

Rhoads, R. E. (1988) *TIBS 13*, 52-56.

Rhoads, R. E. (1991a) *J. Biol. Chem. 268*, 3017-3020.

Rhoads, R. E. (1991b) *Translation in Eukaryotes*, 109-148. CRC Press, Inc., Boca Raton, Fla.

Rhoads, R. E. (1993) *J. Biol. Chem. 266*, 3017-3020.

Rhoads, R. E., Hiremath, L. S., Rychlik, W., Gardner, P. R., and Morgan, J. L. (1985) *The Messenger RNA Cap-binding Protein*, pp 427-464. In E. A. Smuckler and G. A. Clawson (ed.).

Rhoads, R. E., Joshi, B., and Minich, W. B. (1994) *Biochimie 76*, 831-838.

Roman R., Brooker, J. D., Seal, S. N., and Marcus, A. (1976) *Nature 260*, 359-360.

Rozen, R., Edery, I., Meerovitch, K., Dever, T. E., Merrick, W. C., and Sonenberg, N. (1990) *Mol. Cell. Biol. 10*, 1134-1144.

Rychlik, W., Domier, L. L., Gardner P. R., Hellmann, G. M., and Rhoads, R. E. (1987) *Proc. Natl. Acad. Sci. U. S. A. 84*, 945-949.

Sha, M. (1995) "Steady-state and Stopped-flow Fluorescence Measurements of The Interaction of Translational Initiation Factors with mRNA and The Interaction of Transcription Stimulatory Factor USF with DNA", Ph.D. thesis of the City University of New York, pp 25-31.

Sha, M., Wang, Y., Xiang, T., van Heerden, A., Browning, K. S., and Goss, D. J. (1995) *J. Biol. Chem. 270*, 29904-29909.

Shatkin, A. J. (1985) *Cell 40*, 223-224.

Silence, K., D'Hoore, A., Engelborghs, Y., Peyrot, V., and Briand, C. (1992) *Biochemistry 31*, 11133-11137.

Sonenberg, N., Rupprecht, K. M., Hecht, S. M., and Shatkin, A. J. (1979). *Proc. Natl. Acad. Sci. USA 76*, 4345-4349.

Sreerama, N., and Woody, R. W. (1993) *Anal. Biochem., 209*, 32-44.

Stern, O., and Volmer, M. (1919) *Physik Z. **20***, 183-188.

Tahara, S. M., Morgan, M. A., and Shatkin, A. J. (1981) *J. Biol. Chem.**256***, 7691-7694.

Ueda, H., Iyo. H., Doi. M., Inone, M., Ishida, T., Morioka, H., Tanaka, T., Nishikawa, S., and Uesugi, S. (1991a) *FEBS Lett. **280***,207-210.

Ueda, H., Maruyama, H., Doi, M., Inoue, M., Ishida, T., Morioka, H., Tanaka, T., Nishikawa, S., and Uesugi, S. (1991b) *J. Biochem. (Tokyo) **109***, 882-889.

Webb, N. R., Chari, R. V. J., DepPillis, G., Kozarich, J. W., and Rhoads, R. E. (1984) *Biochemistry **23***, 177-181.

van Heerden, A., and Browning, K. S. (1994) *J. Biol. Chem. **269***, 17454-17457.